Nat. Hazards Earth Syst. Sci., 21, 2949–2972, 2021
https://doi.org/10.5194/nhess-21-2949-2021
© Author(s) 2021. This work is distributed under
the Creative Commons Attribution 4.0 License.

Natural Hazards and Earth System Sciences
Open Access
EGU

A climatology of sub-seasonal temporal clustering of extreme precipitation in Switzerland and its links to extreme discharge

Alexandre Tuel[1] **and Olivia Martius**[1,2]

[1]Institute of Geography and Oeschger Centre for Climate Change Research, University of Bern, Bern, Switzerland
[2]Mobiliar Lab for Natural Risks, University of Bern, Bern, Switzerland

Correspondence: Alexandre Tuel (alexandre.tuel@giub.unibe.ch)

Received: 25 March 2021 – Discussion started: 6 April 2021
Revised: 14 September 2021 – Accepted: 15 September 2021 – Published: 1 October 2021

Abstract. The successive occurrence of extreme precipitation events on sub-seasonal timescales can lead to large precipitation accumulations and extreme river discharge. In this study, we analyze the sub-seasonal clustering of precipitation extremes in Switzerland and its link to the occurrence and duration of extreme river discharge. We take a statistical approach based on Ripley's K function to characterize the significance of the clustering for each season separately. Temporal clustering of precipitation extremes exhibits a distinct spatiotemporal pattern. It occurs primarily on the northern side of the Alps in winter and on their southern side in fall. Cluster periods notably account for 10 %–16 % of seasonal precipitation in these two regions. The occurrence of a cluster of precipitation extremes generally increases the likelihood and duration of high-discharge events compared to non-clustered precipitation extremes, particularly at low elevations. It is less true in winter, when the magnitude of precipitation extremes is generally lower and much of the precipitation falls as snow. In fall, however, temporal clusters associated with large precipitation accumulations over the southern Alps are found to be almost systematically followed by extreme discharge.

1 Introduction

Switzerland's climate, topography and high population density make floods one of the major natural disasters, accounting for instance for 71% of weather-related insurance claims over the 1973–2011 period (Swiss Re, 2012) and 36 % of total damages to buildings between 1995 and 2014 (BAFU, 2016). Apart from high Alpine regions where summer snowmelt accounts for a large part of the flood hazard, floods and landslides over much of Switzerland typically follow widespread heavy precipitation (Froidevaux et al., 2015; Froidevaux and Martius, 2016). Large precipitation accumulations may sometimes result from the occurrence of several extreme precipitation events in close succession. In contrast to persistent but moderate wet conditions, temporal clusters of extreme precipitation events involve more than 1 d of extreme precipitation. Such events can lead to extreme river discharge, flash flooding (Doswell et al., 1996) or mass movement, especially in urban and mountain areas (Guzzetti et al., 2007; Panziera et al., 2016). Temporal clustering of extremes also complicates rescue, clean-up and repair efforts (Raymond et al., 2020). Furthermore, clusters of extremes tend to be missing from risk models, which often rely on assumptions of independence in the timing of extreme precipitation occurrence (Priestley et al., 2018).

In Switzerland, several major floods in recent history were linked to series of extreme precipitation events (Barton et al., 2016). In 1993, three events that occurred between 21 September and 15 October led to record 10 to 30 d precipitation accumulations in southern Valais and the Ticino region and caused repeated overflowing of Lake Maggiore above its 100-year return level. Similar conditions around Lake Maggiore were repeated over the course of 4 weeks in fall 2000 and again in November 2002, each time bringing the lake above its critical flooding level. The major August 2005 floods in central Switzerland were likewise connected to a series of heavy rainfall events in the second half of the month (BAFU and WSL, 2008). Recent other examples of temporal clusters of precipitation extremes leading to major floods include the Pakistan floods of summer 2010 (Mar-

source: https://doi.org/10.48350/157400 | downloaded: 17.4.2024

tius et al., 2013), the central Europe floods of summer 2013 (Grams et al., 2014) and the UK floods of winter 2013/14 (Priestley et al., 2017).

Assessing the temporal dependence in the occurrence of extreme precipitation events at the catchment scale is therefore crucial to accurately quantify flood hazard. Such an assessment has not yet been attempted for the whole of Switzerland. Barton et al. (2016) analyzed the sub-seasonal serial/temporal clustering of precipitation extremes in southern Switzerland using a non-parametric approach, Ripley's K function, and found a significant tendency toward clustering during the fall season. They also examined the weather dynamics associated with specific cluster events. At the European scale, Yang and Villarini (2019) quantified the influence of large-scale climate modes on the temporal clustering of extreme precipitation, while Mailier et al. (2006), Vitolo et al. (2009) and Pinto et al. (2013) looked at clustering in winter extratropical storms in the Euro-Atlantic sector, a region where serial cyclone clustering is particularly relevant (Dacre and Pinto, 2020). More recently, Tuel and Martius (2021) attempted a systematic global and seasonal assessment of extreme precipitation temporal clustering at sub-seasonal timescales. Their analysis was however conducted at coarse spatial resolutions relative to the size of Swiss catchments and focused primarily on clustering signals at large spatial scales.

Additionally, few studies have attempted to evaluate the links between extreme discharge or floods and extreme precipitation clusters, and none have conducted such a systematic assessment for Switzerland. The analysis by Barton et al. (2016) focused on selected examples of floods triggered by clusters of extreme precipitation events, as did other studies over Europe (Blackburn et al., 2008; Grams et al., 2014; Huntingford et al., 2014; van Oldenborgh et al., 2015; Priestley et al., 2017; Insua-Costa et al., 2019) or Southwest Asia (Martius et al., 2013). Villarini et al. (2013) considered the temporal clustering of flood events over the American Midwest and its link to large-scale climate patterns, but did not discuss precipitation. Kopp et al. (2021), by contrast, presented a global perspective on the link between sub-seasonal clustering and extremes of cumulative precipitation. In their analysis, however, Switzerland was covered by three to four major catchments only, which prevented a discussion of local variability in the results.

Relationships between extreme precipitation and flood occurrence in Switzerland have been more extensively analyzed. Stucki et al. (2012) and Froidevaux and Martius (2016) both looked at atmospheric precursors of extreme floods, and Giannakaki and Martius (2016) discussed the weather patterns associated with intense precipitation events. Helbling et al. (2006) and Diezig and Weingartner (2007) assessed the role of different flood drivers across Swiss catchments, like extreme or continuous rainfall, rain-on-snow events, and snow and/or glacier melt. Finally, Froidevaux et al. (2015) quantified the influence of accumulated precipitation before annual peak discharge events across 101 Swiss catchments. They showed that short-range antecedent precipitation, up to 3 d before an event, was the most relevant predictor of peak discharge occurrence and magnitude. Long-range antecedent precipitation, from 4 d to a month before an event, was nevertheless still relevant for the Jura mountains and parts of the Swiss Plateau. However, it is unclear whether these conclusions still hold in the case of prolonged or recurrent high-discharge conditions, characterized by repeated exceedances of daily discharge percentiles over short time windows. The hydrological response to multiple extreme precipitation events occurring as part of a cluster may also differ from the response to the same events separated by longer time periods. Paschalis et al. (2014) indeed showed that discharge peaks were strongly shaped by antecedent soil wetness conditions, themselves largely affected by the temporal correlation of precipitation. In addition, in basins with high retention capacities (e.g., with natural or artificial lakes), single extreme precipitation events may not be enough to trigger extreme discharge, unlike prolonged periods of heavy precipitation.

The goals of this study are therefore twofold. First, we aim to quantify the sub-seasonal clustering of precipitation extremes in time across Switzerland using several gridded station- and satellite-based datasets. We take the same approach as Barton et al. (2016) and Tuel and Martius (2021) which relies on Ripley's K function as an indicator of clustering, and we analyze each season separately to remove the seasonal signal in extreme precipitation magnitude. We then discuss the patterns and robustness of the spatiotemporal distribution of sub-seasonal clustering in Switzerland. Second, we evaluate the links between extreme precipitation clusters, extreme precipitation accumulations and extreme discharge using observed discharge data at 93 gauges across Switzerland. After introducing the data and methods used in this study, we briefly discuss the seasonality of extreme precipitation and discharge magnitude across Switzerland, before moving on to results and their discussion.

2 Data and study area

2.1 Data

2.1.1 Precipitation

Reference precipitation data for this study come from the daily 2×2 km RhiresD dataset. RhiresD, developed by MeteoSwiss, covers the period from 1961 to present. It is obtained by spatial interpolation of data from a high-density rain-gauge network that extends across Switzerland, with at least 420 stations available for any single day. The effective scale of RhiresD varies as a function of station density but is on average of the order of 15–20 km, the typical inter-station distance. A detailed description of this dataset can be

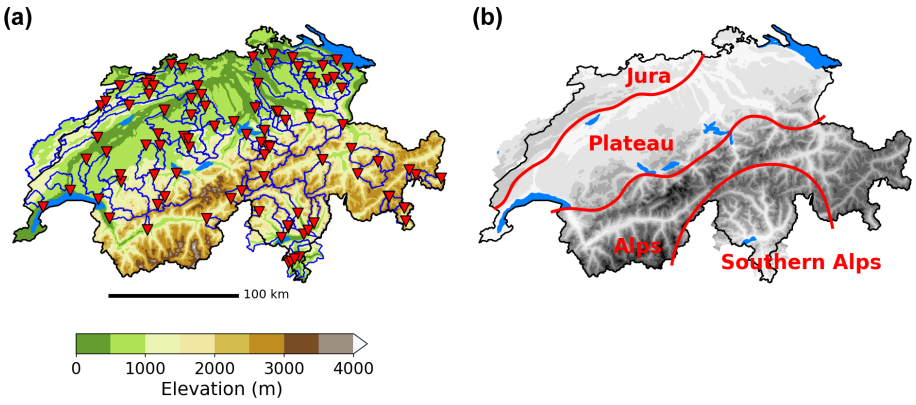

Figure 1. **(a)** Topography of Switzerland (shading, with major lakes shown in light blue) and gauged catchments used in this study (catchment boundary: blue lines; catchment gauge location: red triangles). The thick black line indicates the Swiss border. **(b)** Switzerland's topography (shaded) and major climate and hydrological regions (red).

found at https://www.meteoswiss.admin.ch/home/climate/swiss-climate-in-detail/raeumliche-klimaanalysen.html (last access: 1 October 2021), and the interpolation algorithm is described in Frei and Schär (1998).

For purposes of comparison, we also consider other daily precipitation datasets, at their native resolutions: ERA5 (Hersbach et al., 2020), the latest ECMWF reanalysis available from 1979 onwards at 0.25° resolution, in which precipitation is a forecasted quantity, i.e., not directly constrained by assimilated observations; the satellite-based TRMM TMPA (TRMM Multi-Satellite Precipitation Analysis) 3B42 version 7 (50° S–50° N, 1998–2019, 0.25° resolution) (Huffman et al., 2007); CMORPH (60° S-60° N, 2003–2019, 0.25° resolution) (Joyce et al., 2004); and the land-only, station-based Climate Prediction Center Global Unified Gauge-Based Analysis of Daily Precipitation (1979–2019, 0.5° resolution) (Chen et al., 2008) and EOBS gridded product version 19.0e (1950–2019, 0.25° resolution) (Haylock et al., 2008).

2.1.2 Discharge observations

We analyze daily discharge observations for 93 small to medium-sized gauged catchments (14–1700 km^2) distributed across Switzerland (Fig. 1a). The catchments cover a wide variety of catchment characteristics and climates, from glacial and nival runoff regimes at high altitudes to pluvial regimes in the Swiss plateau (see Table A1 for catchment characteristics). These catchments were analyzed by Muelchi et al. (2021a), who selected them based on several criteria: data availability, the absence of major lakes, minimal human influence and satisfactory calibration results in their hydrological model. The data for each catchment range from January 1961 to December 2017 (Table A1); the proportion of catchments with data rises from about 45% in the early 1960s to more than 95 % in 1995, at which level it remains until 2015, before rapidly decreasing to 30 % by the end of 2017. For each catchment, the analysis is conducted over the period for which discharge data are available. This means that daily discharge percentiles (and precipitation percentiles, when precipitation and discharge are considered together) are calculated over different time periods depending on the catchment.

2.1.3 Catchment-scale aggregation

We average RhiresD data over a hydrological partitioning of Switzerland that consists of 63 catchments with a mean area of 900 km^2 (see Fig. 4). Catchment-scale aggregation is useful to identify the occurrence of high-impact heavy-precipitation events and also to smooth RhiresD data to a lower resolution more consistent with its effective resolution. Though we could also use the set of 93 gauged catchments, this set does not cover the whole of Switzerland. Consequently, we opt for a countrywide partitioning of 63 larger catchments (for which no discharge observations are available). To be comprehensive and to help compare results between discharge and precipitation, we also show the results obtained for the 93-catchment set in the appendix (Figs. A4–A6).

2.2 Study area

Switzerland can be divided into several regions with distinct climates and hydrological regimes: the Jura, the Plateau, the Alps and the southern Alps (Fig. 1b) (Umbricht et al., 2013; Aschwanden and Weingartner, 1985). These regions notably exhibit quite different seasonal cycles in extreme precipitation and discharge occurrence. In the Plateau, the heaviest precipitation occurs chiefly during summer (Fig. 2c) (Helbling et al., 2006; Diezig and Weingartner, 2007; Panziera et al., 2018), as a result of convective instability (Stucki et al., 2012), frequent westerly winds and Atlantic water vapor transport (Giannakaki and Martius, 2016). In summer, how-

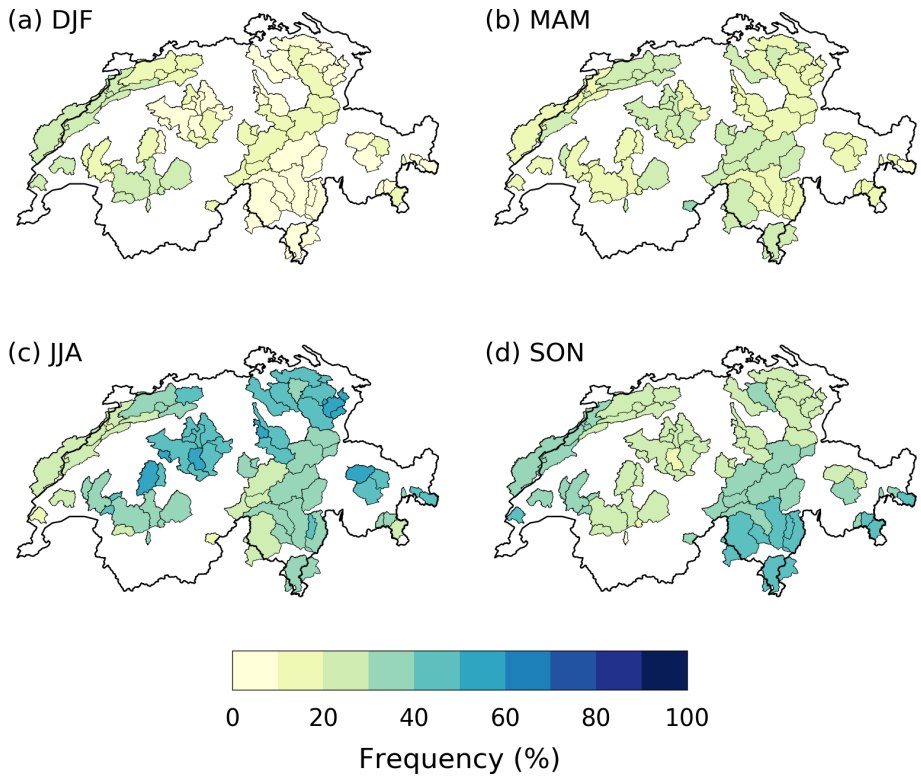

Figure 2. Seasonal frequency of exceedance of annual 99th daily precipitation percentile in RhiresD: **(a)** DJF, **(b)** MAM, **(c)** JJA and **(d)** SON.

ever, evapotranspiration is highest and soils are less saturated than in the cold season. Consequently, extreme-discharge events are about equally likely to occur in winter, spring and summer (Fig. 3). In the Jura, while the magnitude of extreme precipitation events still peaks in summer, its seasonality is less pronounced. About 20 % of extreme precipitation events indeed occur in winter and spring each (Fig. 2), triggered by forced orographic ascent of moist westerlies (Froidevaux and Martius, 2016). Extreme discharge, however, is mostly confined to winter and spring, largely driven by rain-on-snow processes (Diezig and Weingartner, 2007; Helbling et al., 2006; Köplin et al., 2014).

As in the Jura, the seasonal cycle in extreme precipitation occurrence over the Alps is not strong (Fig. 2) (Frei and Schär, 1998; Umbricht et al., 2013). The peak is reached in summer and fall for most catchments, when extreme precipitation occurs as a result of local convective instability (Stucki et al., 2012), but winter and spring still concentrate 30 %–40 % of extreme events. The outlook for discharge is very different, however. Alpine catchments, especially at high elevations, are mainly driven by snowmelt and glacier melt (Aschwanden and Weingartner, 1985). Thus, extreme discharge is almost exclusively confined to summer (Fig. 3c) (Köplin et al., 2014; Muelchi et al., 2021b). Finally, the southern Alps experience extreme precipitation mostly during summer and fall (Fig. 2c and d) (Frei and Schär, 1998; Isotta et al., 2014). Such behavior results from the frequent southerly advection of moist Mediterranean air caused by upper-level troughs (Barton et al., 2016). These atmospheric conditions are connected to potential vorticity streamers or cut-offs centered west of the Alps, which are most frequent during fall (Martius et al., 2006). Extreme discharge in this region also occurs primarily during fall (50 %–60 % of events; Fig. 3d).

3 Methods

A summary of the methodology adopted in this study is shown in Fig. A1.

3.1 Precipitation and discharge extremes

For each dataset, precipitation extremes are defined on a monthly basis as days when daily accumulated precipitation exceeds the 99th percentile of the corresponding month. For instance, January precipitation values are compared to the January 99th percentile. The percentiles are calculated using all days (both with and without precipitation). Potential trends in extreme daily precipitation percentiles are not taken into account. As the individual weather systems associated with extreme precipitation may sometimes last for several days, we remove the short-term temporal dependence in the occurrence of extreme precipitation events by applying a standard run declustering procedure (Coles, 2001) with a run length of 2 d, well-suited for Switzerland (Barton et al.,

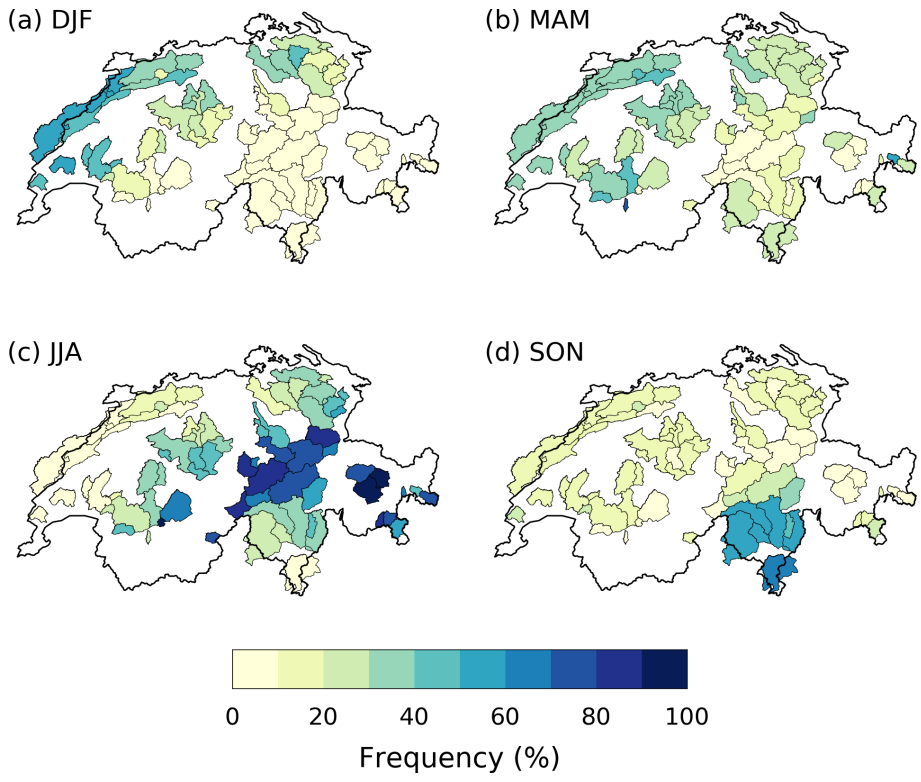

Figure 3. Seasonal frequency of exceedance of annual 99th daily discharge percentile: **(a)** DJF, **(b)** MAM, **(c)** JJA and **(d)** SON.

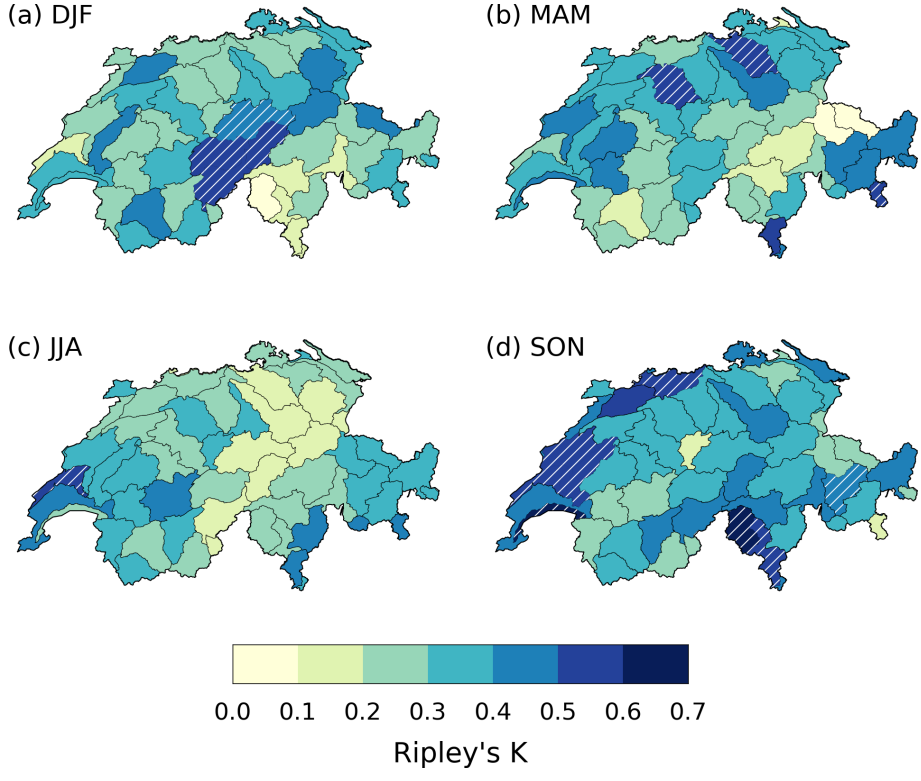

Figure 4. Value of Ripley's K in the RhiresD dataset for a 20 d window (shaded) and clustering significance for a time window of 15–25 d (white hatching) in **(a)** DJF, **(b)** MAM, **(c)** JJA and **(d)** SON.

2016). The goal of the declustering is to remove short-term dependence and to identify independent events. This procedure is for example applied prior to a peak-over-threshold statistical analysis. The declustering merges extreme events that are separated by less than 2 d into a single event. Consequently, it reduces the number of extreme events compared to the original series. Events within each season (winter: DJF; spring: MAM; summer: JJA; and fall: SON) are then analyzed together.

Extreme-discharge events for each of the 93 gauged catchments are defined as days when daily discharge exceeds its 95th or 99th percentile calculated on the whole time series (both percentiles are analyzed separately). We look at two extreme percentiles to test the sensitivity of our results to the choice of threshold and also to increase the number of detected high-discharge events. The persistence in extreme-discharge conditions is assessed by identifying periods of persistent high discharge over sub-seasonal timescales. These are defined as periods of length L containing at least N extreme-discharge days. Three sets of (L, N) values are considered: (10,5),(20,8) and (30,10). Depending on the values of L and N, no periods may be found in some catchments, in which case they are simply excluded from the corresponding analysis.

Three reasons justify the choice of seasonally varying thresholds for precipitation and fixed thresholds for discharge. First, such a choice removes the influence of the seasonality in extreme precipitation magnitude. The occurrence rate of extreme precipitation events is therefore constant across the year, and detecting clustering significance is straightforward (see below). Second, impacts of discharge extremes are usually related to their absolute rather than relative magnitude. Third, the seasonal cycles of extreme precipitation and discharge magnitudes are not in phase over much of Switzerland (Figs. 2 and 3). The most extreme discharge does not necessarily occur after the heaviest precipitation events. Surface conditions, like soil saturation, presence of snow/ice, vegetation cover or evaporative demand, considerably shape the discharge response to heavy precipitation (Paschalis et al., 2014). As they vary substantially from one season to the next, the discharge response to the same precipitation magnitude may differ depending on the season.

3.2 Sub-seasonal temporal clustering of precipitation

Temporal clustering of precipitation extremes is quantified with Ripley's K function (Ripley, 1981). Here we give a quick overview of the methodology and refer the reader to Tuel and Martius (2021) for further details. For a given window size w, Ripley's K function applied to a time series measures the average number of extreme events in a neighborhood of w days before and after a random extreme event in the series. This gives information about the tendency towards temporal clustering in the series. The larger the value of Ripley's K function for a given w, the more clustered the extreme events. The significance of temporal clustering in the series is then assessed by comparing Ripley's K values to those obtained from a Monte Carlo sample of 5000 simulated homogeneous Poisson processes with the same average event density as the observed series. In homogeneous Poisson processes, events occur independently from each other and therefore exhibit complete temporal randomness. Because we chose monthly percentiles to define extreme precipitation events, the occurrence rate of extremes is constant throughout the year. Thus we can test for clustering significance against homogeneous series. Non-homogeneous (and more complex) series would have been required if the likelihood of extreme event occurrence has been a function of time.

From this comparison we get an empirical p value for each w. As we deal with multiple hypothesis tests, we implement a false discovery rate procedure (Wilks, 2016) with a baseline significance level of 5 % to identify catchments where clustering is significant. Clustering significance is assessed for two intervals of w values, characteristic of sub-seasonal timescales: 15–25 and 25–35 d. Clustering is said to be significant for a given interval if it is significant for at least half of the w values in that interval.

3.3 Identification of cluster events

We identify extreme precipitation cluster events over 21 d time windows with the algorithm of Kopp et al. (2021) (see their Figs. 3 and 4). Starting from the declustered binary extreme event series, the first step is to calculate the 21 d moving sum of extreme event counts. In a second step, we select the 21 d period with the largest event count (i.e., the highest number of extreme events), if that count is larger than 2. Otherwise, no clusters are found and the algorithm stops. In the case of multiple 21 d periods with the same extreme event count, the one with the largest precipitation total is selected first. In the third step, we remove from the binary event series the extreme events that occur in the selected 21 d period. The algorithm is then run again from the first step onwards to identify the next cluster event. This procedure avoids any overlap between cluster events. The choice of the 21 d time window is well-suited to quantify clustering at sub-seasonal timescales and is generally consistent with the length of observed cluster episodes that led to major floods in Switzerland (see introduction). Results do not differ significantly for slightly shorter or longer (2–4 weeks) windows (see also Kopp et al., 2021).

We then characterize clusters of precipitation extremes with two metrics related to their potential impact. The first is the average contribution of cluster periods to seasonal precipitation. This contribution increases with the frequency and total precipitation of cluster periods. The second metric is the frequency of cluster periods during extreme 21 d precipitation accumulations. It gives an idea of how often cluster periods are responsible for extreme precipitation accumulations,

a frequent trigger of flood events in Switzerland (Froidevaux et al., 2015).

3.4 Effects of temporal clustering of extreme precipitation on the occurrence and duration of extreme discharge

We analyze the influence of clusters of precipitation extremes on discharge in two ways: by looking at discharge characteristics after clusters of precipitation extremes and at precipitation characteristics before persistent high-discharge periods.

First, we calculate for each catchment the probability p_1 of extreme discharge for all days during and up to 5 d after 21 d clusters of precipitation extremes. We also calculate the probability p_2 of extreme-discharge days for periods of the same length and same time of the year as the selected cluster periods. We can then define an odds ratio of extreme-discharge occurrence after clusters of extremes as $\frac{p_1(1-p_2)}{p_2(1-p_1)}$ (Wilks, 2019). The odds ratio compares the likelihood of extreme-discharge occurrence in the presence of a precipitation cluster to its likelihood in the absence of a precipitation cluster. The higher it is, the stronger the relationship between the occurrence of extreme discharge and precipitation clusters. From the identification of 21 d cluster periods, precipitation extremes can also be separated into "clustered" and "non-clustered" events. We then look at the likelihood of extreme-discharge occurrence after both types of events to highlight potential differences in the discharge response.

Second, for each of the persistent high-discharge periods identified as described previously, we calculate the number of precipitation extremes and the percentile of total accumulated precipitation over a window stretching from 10 d before the beginning of the persistent high-discharge period to its end. We choose to begin 10 d before because Froidevaux et al. (2015) showed that moderate wet conditions occurred in the week preceding many flood events in Switzerland, hence the need to look beyond the few days preceding persistent high-discharge periods.

4 Results

4.1 Spatiotemporal patterns of clustering significance

We now turn to the analysis of Ripley's K values and their implications in terms of sub-seasonal temporal clustering. Several coherent areas exhibit K values that are significantly larger than those expected for homogeneous Poisson processes with no temporal dependence (Fig. 4). In winter, significant temporal clustering of precipitation extremes is mainly found in central Switzerland, along the Alpine ridge, at the 15–25 and 25–35 d timescales (Figs. 4a and A2b). In spring, two catchments in northern Switzerland as well as a few catchments in southeastern Switzerland also exhibit significant clustering (Figs. 4b and A2d). By contrast, results for the summer season show a complete absence of temporal clustering significance at all timescales (Figs. 4c and A2e, f). Finally, in fall, significance is found at all timescales over both the western tip of Switzerland and the southern side of the Alps (Figs. 4d and A2g, h).

Similar patterns are found by comparing to the coarser-resolution precipitation datasets (ERA5, TRMM, EOBS, CPC and CMORPH), with some notable exceptions. Clustering significance over the Alps in winter is also present in the coarser-resolution data, but with a wider extent than in RhiresD (Fig. 5a; see also Fig. A3). Temporal clustering during spring is generally less significant across Switzerland (Fig. 5b). Two datasets indicate significant clustering locally in northwestern Switzerland, but none do along the northern and southern borders where significance was found in RhiresD. By contrast, all datasets agree on the absence of clustering in summer (Fig. 5c), and on significant clustering in southern and southeastern Switzerland during the fall season (Fig. 5d). Temporal clustering does not appear particularly significant, however, in western Switzerland during fall. In winter, clustering significance extends over a large region stretching from the Mont Blanc massif in France to eastern Switzerland along the Alpine ridge, in good agreement with RhiresD (Figs. 4a and 5a). Similarly, southern Switzerland is part of a larger region exhibiting significant clustering, encompassing northern Lombardy and possibly extending southwards to the Mediterranean shore (Fig. 5d).

4.2 Characteristics of cluster events

We now expand the statistical analysis by showing the characteristics of clustered precipitation events. In winter, extreme precipitation clusters contribute an average of $\approx 10\,\%$ to total winter precipitation along the Alpine ridge where clustering is statistically significant (Fig. 6a). Additionally, clusters occur during about 60 %–70 % of extreme 21 d precipitation accumulations (above the corresponding 99th percentile) (Fig. 7a). Elsewhere, clusters contribute little to both seasonal and extreme precipitation accumulations. In spring, the average contribution of clusters to seasonal precipitation is overall weak ($< 10\,\%$), even for catchments where clustering in RhiresD is statistically significant (Fig. 6b). Yet, over western Switzerland, periods of extreme 21 d accumulations are almost always cluster periods as well (Fig. 7b). In summer, consistent with the absence of clustering at that time of the year, clusters do not contribute much to seasonal precipitation. Finally, in fall, cluster contribution to seasonal precipitation reaches its annual maximum of 12 %–16 % over southeastern Switzerland (particularly the southern Alps). It is also quite high ($\geq 10\,\%$) over western Switzerland where clustering is statistically significant as well (Fig. 6d). In addition, more than 80 % of extreme precipitation accumulation periods are accompanied by cluster events in the southern Alps (Fig. 7d). Since extreme discharge in this area is most common during fall (Fig. 3d), this suggests a possibly im-

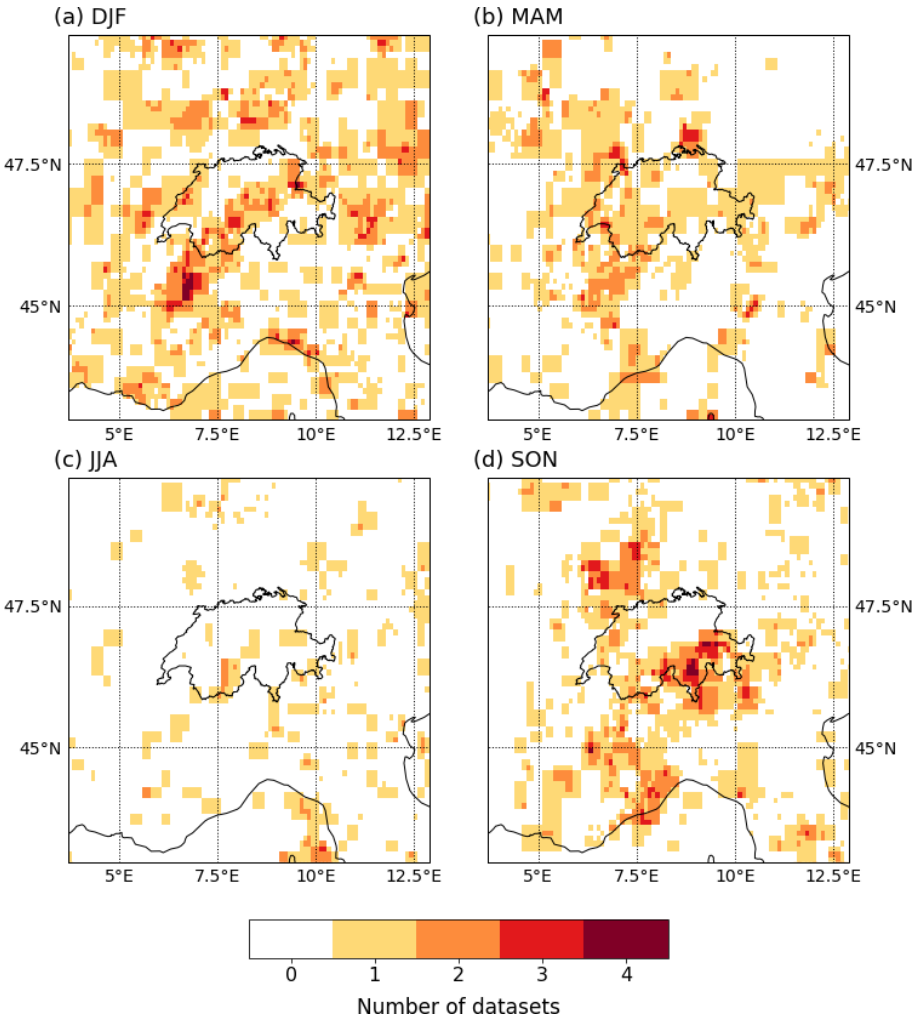

Figure 5. Number of datasets (among ERA5, TRMM, CMORPH, CPC and EOBS) that agree on the significance of extreme precipitation clustering for a 15–25 d window in **(a)** DJF, **(b)** MAM, **(c)** JJA and **(d)** SON. For this comparison, all datasets were regridded to the smallest 0.1° EOBS resolution.

portant role of extreme precipitation clusters in high-impact weather events in this region and at that time of the year.

4.3 Discharge response to extreme precipitation clustering

Persistent high-discharge periods, regardless of L and N values, are systematically associated with extreme precipitation accumulations for catchments with mean elevations up to about 1500 m (Figs. 8a, b and 9a). Above 1500 m, glacial/nival runoff regimes dominate, and the link to extreme precipitation accumulations is weaker. By contrast, extreme precipitation clusters precede persistent high-discharge periods only in the southern Alps and locally over the eastern parts of the Swiss Plateau and the Jura (Fig. 8c and d). The dependence on catchment elevation is similar, with a much weaker intersection of cluster events and extreme discharge at high elevations, but less robust with a larger spread of values at low elevations (Fig. 9b).

For most catchments, particularly those below 1500 m elevation, the discharge response after an extreme precipitation event differs between single extreme events and events that are part of clusters (Fig. 10). In the 5 d following an extreme precipitation event, the fraction of days exceeding either the 95th or the 99th percentile of daily discharge is higher when that event belongs to a cluster. The difference is particularly large over northern Switzerland and in the southern Alps where, for instance, the 99th percentile of daily discharge values is exceeded on average 20 %–30 % of the time (1–1.5 d) in the 5 d following an extreme precipitation event during a cluster but only 10 %–15 % of the time if the extreme occurred outside of a cluster. Given that daily discharge exceeds its 99th percentile on average only ≈ 3.5 d a year, this implies an important effect of clustered extremes.

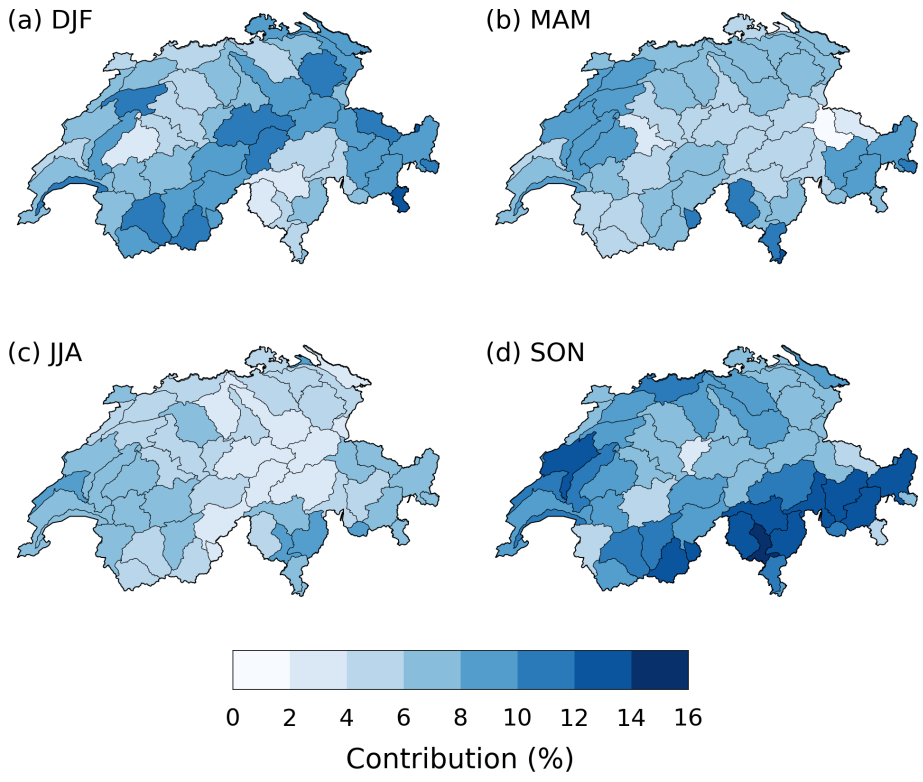

Figure 6. Contribution of 21 d extreme precipitation clusters to seasonal precipitation in RhiresD, in **(a)** DJF, **(b)** MAM, **(c)** JJA and **(d)** SON.

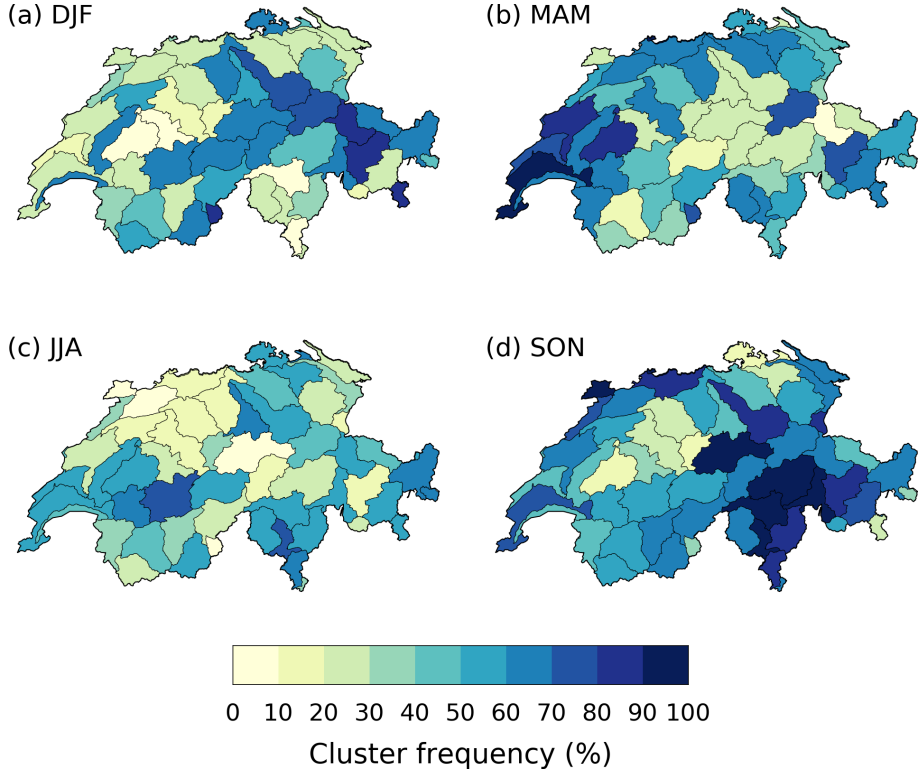

Figure 7. Frequency of extreme precipitation cluster occurrence during extreme 21 d cumulative precipitation events (> 99th percentile) in RhiresD, in **(a)** DJF, **(b)** MAM, **(c)** JJA and **(d)** SON.

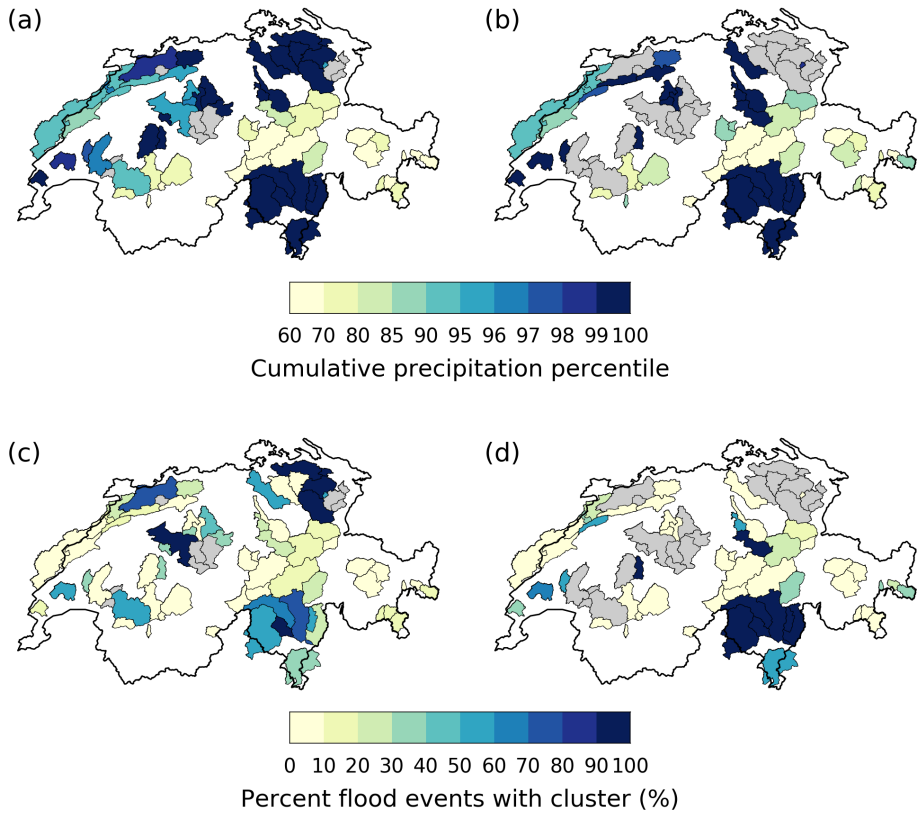

Figure 8. **(a, b)** Average cumulative precipitation percentile during and 10 d prior to persistent high-discharge periods, defined as **(a)** at least 5 d within a 10 d window with discharge above its 99th percentile and **(b)** at least 8 d within a 20 d window with discharge above its 99th percentile. Catchments for which such persistent high-discharge periods are not observed are shown in gray. **(c, d)** Same as **(a, b)**, but for the frequency of cluster occurrence during and 10 d prior to persistent high-discharge periods.

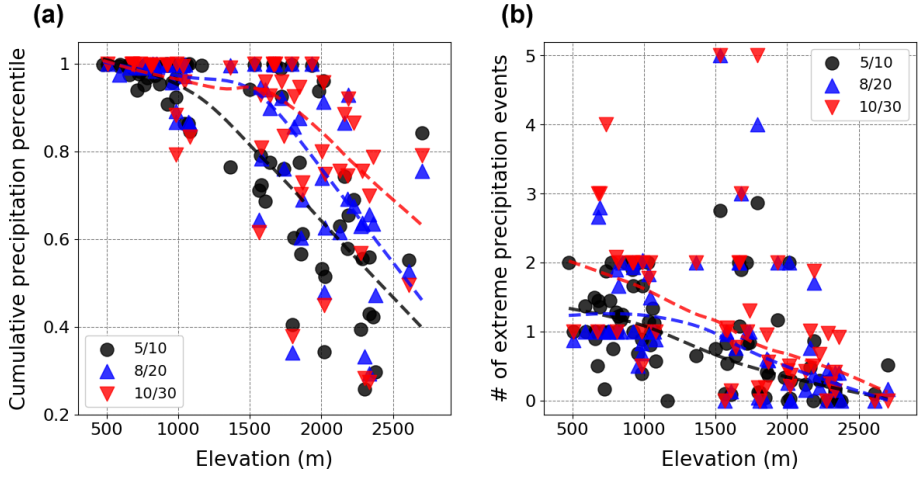

Figure 9. **(a)** Average cumulative precipitation percentile during and 10 d prior to persistent high-discharge periods as a function of mean catchment elevation. Black circles (respectively blue triangles, red triangles) correspond to events characterized by at least 5 d (respectively 8, 10 d) within a 10 d (respectively 20, 30 d) window with discharge above its 99th percentile. **(b)** Same as **(a)**, but for the number of extreme precipitation events.

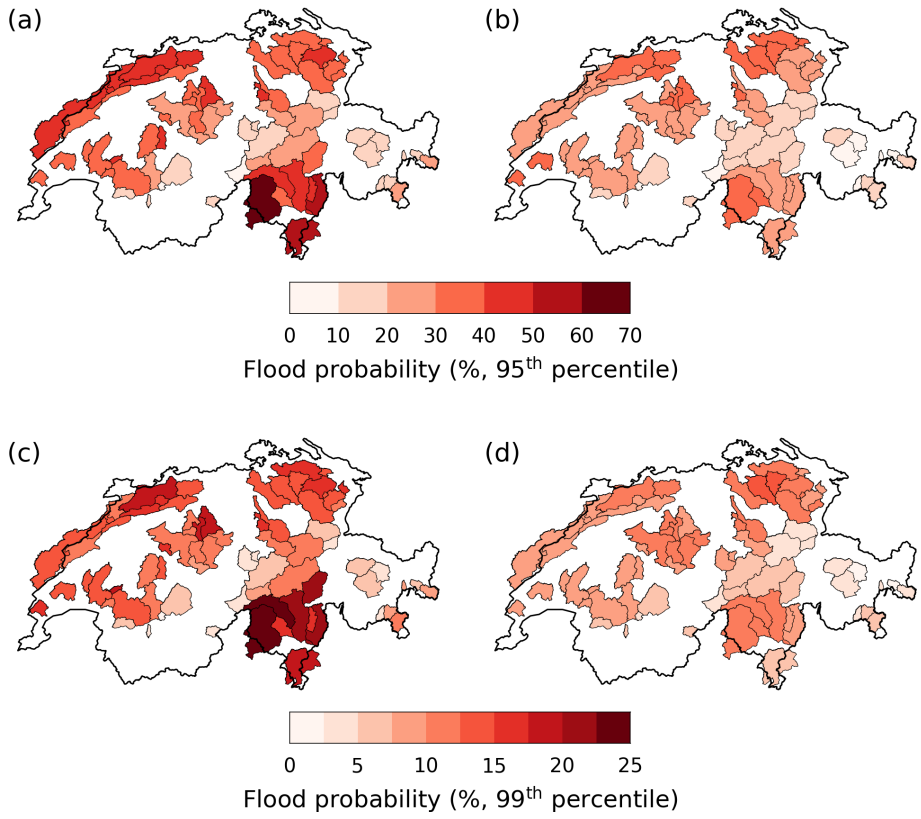

Figure 10. **(a, b)** Fraction of days with discharge above its 95th percentile in the 5 d following **(a)** an extreme precipitation event that is part of a 21 d cluster and **(b)** any random precipitation extreme. **(c, d)** Same as **(a, b)** but for the 99th daily discharge percentile.

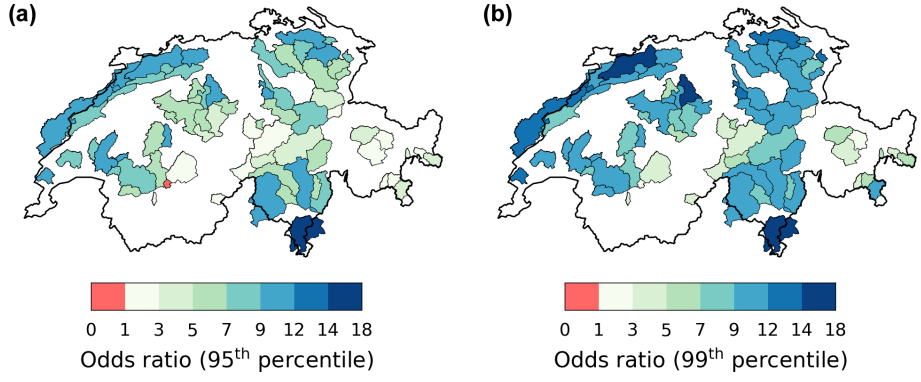

Figure 11. Odds ratio for extreme-discharge occurrence (defined based on daily **(a)** 95th and **(b)** 99th discharge percentiles) during and up to 5 d after cluster events (see Sect. 3.4 for methodological details).

The occurrence of a cluster of precipitation extremes greatly increases the likelihood of high-discharge events, particularly at low elevations, as evidenced by high odds ratio values (Fig. 11). Daily discharge is more than 7 (10) times more likely to exceed its 95th (99th) percentile during and after a cluster in the Jura, for instance. The distribution of daily discharge percentiles after extreme precipitation events confirms these results: while the probability of exceeding high-discharge thresholds on the day following an extreme event is not very different between clustered and non-clustered extremes, that probability decreases much faster in the days following non-clustered extremes (Fig. 12).

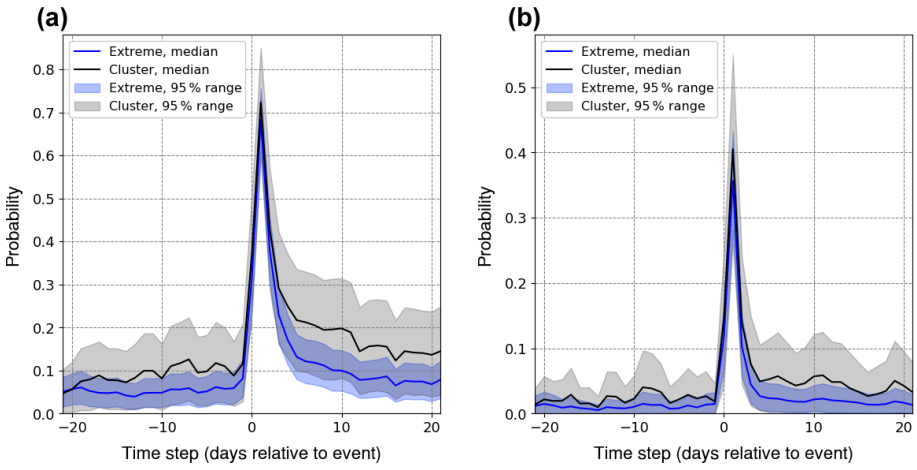

Figure 12. Probability of exceeding the **(a)** 95th and **(b)** 99th percentiles of daily discharge around an extreme precipitation event that is part of a 21 d cluster (black) and around any random precipitation extreme (blue) across catchments with a mean elevation smaller than 1500 m. Solid lines correspond to the multi-catchment median and shading to the 95 % range.

5 Discussion

5.1 Patterns of clustering significance and their physical interpretation

Our definition of extreme precipitation events based on the exceedance of monthly percentiles of daily precipitation removes the influence of seasonality in extreme precipitation magnitude (Fig. 2). By applying Ripley's K function to the resulting time series, we can thus focus on short-term temporal dependence in extreme precipitation occurrence driven by sub-seasonal dynamics or intra-annual variability (e.g., climate modes). Clustering significance is found mainly over the Alps during winter and in southern and southeastern Switzerland during fall (Figs. 4 and A2). The spatial coherence and robustness of the results over these two regions across timescales and datasets (Fig. 5) suggests that specific physical processes are responsible for the clustering.

Both in winter and in fall, clustering significance is chiefly concentrated at timescales below 30 d, which seems to preclude any dominant role of seasonal sea-surface temperature anomalies (Tuel and Martius, 2021).

First, we discuss the spatial pattern during winter, when significant clustering occurs in the central Alps. During winter, extreme precipitation events in northern Switzerland often occur in connection with extreme integrated water vapor transport (e.g., linked to atmospheric rivers) that interacts with the orography (Piaget et al., 2015; Froidevaux and Martius, 2016; Giannakaki and Martius, 2016). The concentration of clustering significance over the Alps during winter possibly results from a spatial anchoring of precipitation at high elevations, through orographic lifting and convergence of the moist air masses, while precipitation in the lower-lying area is spatially more dependent on the presence of cold-air pools upstream of the mountains (Medina and Houze, 2003; Rössler et al., 2014; Piaget, 2015). The spatial extent of these cold pools may vary from event to event, along with the location of the strongest precipitation.

Next, we discuss the spatial pattern during fall when clustering occurs south of the Alps. During fall, several major clusters of precipitation extremes south of the Alps were related to recurrent Rossby wave breaking over western and southwestern Europe (Barton et al., 2016). The wave breaking leads to enhanced low-level moisture transport from the Mediterranean towards the Alps (Martius et al., 2006; Barton et al., 2016). Barton et al. (2016) discuss why wave breaking was recurrent for four case studies. Recurrent cyclogenesis and extratropical transition of tropical cyclones upstream over the western Atlantic seem to play a role, but not necessarily a systematic one. Persistence in blocking conditions in the northwestern Atlantic also contributed to upper-level wave amplification and the subsequent occurrence of extreme-precipitation clusters in southern Switzerland (Barton et al., 2016).

The apparent lack of agreement among precipitation datasets regarding the significance of the clustering over western Switzerland in fall (Figs. 4d and 5d) is less straightforward to interpret. Despite the precautions taken to control the false discovery rate, it is still possible that significance in this region is detected by pure chance. Yet, it is not altogether obvious that the gridded satellite or reanalysis datasets are completely reliable either. If thunderstorms are responsible for many extreme precipitation events, their representation in reanalysis products can be questioned. Their small spatial scale may also cause them to be missed in satellite products. While coarse-resolution gridded datasets seem to agree on the timing and magnitude of precipitation extremes in western Switzerland during fall (Rivoire et al., 2021), a more detailed comparison with RhiresD data and an analysis

of the type of events responsible for these extremes would be required to conclude.

5.2 Relevance of extreme precipitation clusters for flood hazard

Persistent high-discharge periods at elevations lower than 1500 m a.s.l. are almost systematically associated with extreme precipitation accumulations in the preceding days (Fig. 8a and b). This is consistent with the mainly pluvial regimes at lower elevations, as well as with the results of Froidevaux et al. (2015). Such accumulations are not always the consequence of clusters of extremes, however. Outside southern Switzerland during fall, western Switzerland during spring and, to a lesser extent, Alpine catchments during winter, the overlap of cluster events and extreme precipitation accumulations is generally smaller than 50 %, and often smaller than 25 % (Fig. 7). Results in summer and spring can be understood by the scarceness of cluster events in those seasons. In winter, despite being frequent, clusters over the Alps are less systematically associated with extreme accumulations, which are often the result of a single heavy-precipitation event.

Still, from the perspective of surface impacts, clusters remain relevant, regardless of their overall frequency, if they increase flood hazard. The discharge response to both clustered and non-clustered extreme precipitation events typically peaks 1 d after the event (Fig. 12), consistent with the findings of Froidevaux et al. (2015). However, our results show that clusters of precipitation extremes increase the likelihood of occurrence and the duration of high-discharge events, particularly at low elevations (Figs. 10 and 11). This influence is noticeably larger than for non-clustered precipitation extremes (Fig. 12). On average, daily accumulated precipitation during clustered and non-clustered extremes is similar. Instantaneous precipitation rates might be different, but it is not possible to verify it given the daily resolution of the precipitation data. However, the first extreme in a cluster event likely increases soil moisture, which enhances the discharge response to the subsequent precipitation extremes (Merz et al., 2006; Nied et al., 2014; Paschalis et al., 2014). The role of antecedent soil moisture in flood generation and volume is well-documented for Switzerland and Alpine catchments (e.g., Keller et al., 2018). This may explain why extreme-discharge probability decreases more slowly after clustered precipitation extremes compared to non-clustered events (Fig. 12).

This difference is quite high in the southern Alps (e.g., Fig. 9c and d), possibly due to the fact that floods in this area generally occur in the fall (Fig. 3d; Barton et al., 2016) when clusters bring substantial amounts of precipitation (Fig. 7d). There, frequent clusters leading to extreme precipitation accumulations are likely to be an important precursor of major flood events, as confirmed by observations of several damaging clustering periods (Barton et al., 2016). This region of Switzerland also experiences the largest precipitation extremes (Umbricht et al., 2013). Additionally, it is characterized by poor infiltration rates, steep slopes and weak soils (Aschwanden and Weingartner, 1985). Infiltration excess (connected to Hortonian-type storm runoff generation) may therefore be more rapidly reached than in the rest of the country. Coupled with saturation excesses following the first extreme event in a cluster, it might explain why the region stands out in most of our analyses.

By contrast, in the Alps during winter, though clustering is statistically significant, its impact on extreme discharge is quite limited. This results most likely from the fact that discharge in Alpine catchments is lowest in winter, when much of the precipitation falls as snow and the magnitude of precipitation extremes is generally lower.

Finally, the case of western Switzerland during spring is interesting. Though rare, clusters are responsible for almost all extreme precipitation accumulations (Fig. 7b). Over this region, floods are somewhat less frequent in spring than in winter (Fig. 3a and b), despite similar extreme precipitation likelihood (Fig. 2a and b). This may result from fewer rain-on-snow events, a major flood process for the region (Aschwanden and Weingartner, 1985; Köplin et al., 2014), but also drier soils coupled to high infiltration rates (Aschwanden and Weingartner, 1985). Yet, spring floods can still be quite devastating, since precipitation generally falls as rain instead of snow, and limited vegetation cover makes erosion more likely. Consequently, cluster events that affect western Switzerland during spring should be the focus of further research.

5.3 Some limitations and future prospects

Our approach to quantify links between clustered extremes and flood response has a number of limitations. First, we based our analysis on the exceedance of given precipitation and discharge percentiles, not taking into account either flood volumes or precipitation intensities. This is naturally quite restrictive and in particular fails to capture potential non-linearities in relationships above the selected percentiles. In addition, spatial variability in extreme discharge or average total cluster precipitation were not analyzed.

Our results only focus on the hazard component of flood risk. We do not take into account exposure and vulnerability, which may differ substantially between catchments due to variability in population density, infrastructure, flood management capacities, etc. Similarly, we did not take into account the influence of catchment regulation in this work. While the analyzed catchments are generally not heavily regulated ones, human influence may still be felt, especially when it results in the smoothing over time of extreme-discharge conditions, which would impact our analysis of persistent flood events.

Finally, our definition of floods and flooding persistence was also somewhat simplistic. First, while from the perspec-

tive of impacts it makes sense to define floods based on annual discharge percentiles, in snow-driven or glaciated catchments, this choice may discard potential high-discharge conditions occurring outside summer. Second, our definition of flooding persistence based on a minimal number of flood days in a given time window lumps together single, long floods and recurrent short ones, two kinds of events with potentially different impacts, and which may have to be managed differently.

6 Conclusions

The main findings of this study are as follows. First, we identified a specific seasonal and spatial pattern of significance in sub-seasonal temporal clustering of extreme precipitation events across Switzerland. Various station- and satellite-based datasets point to generally significant clustering over the Alps in winter, particularly their central part, and over southern Switzerland during fall. Second, extreme precipitation clusters play a contrasted role in seasonal and sub-seasonal extreme precipitation accumulations. Their contribution is particularly high in fall over southern Switzerland, but more limited over the Alps in winter. Clusters are also frequently associated with extreme precipitation accumulations over western Switzerland during spring, despite their relative scarcity. Finally, cluster events, regardless of their frequency, are generally associated with a higher flood likelihood and more persistent flood conditions over much of Switzerland. The southern Alps region stands out from this analysis. There, clusters of precipitation extremes are frequent during fall and tend to bring particularly large amounts of precipitation. As a result, they appear to be critical precursors of major flood events, a conclusion supported by previous event-based analyses. While our results are exclusively focused on Switzerland, the method adopted for this analysis could in principle be applied to other regions of the world to quantify the relevance of temporal heavy-precipitation clusters for flood hazard.

Appendix A

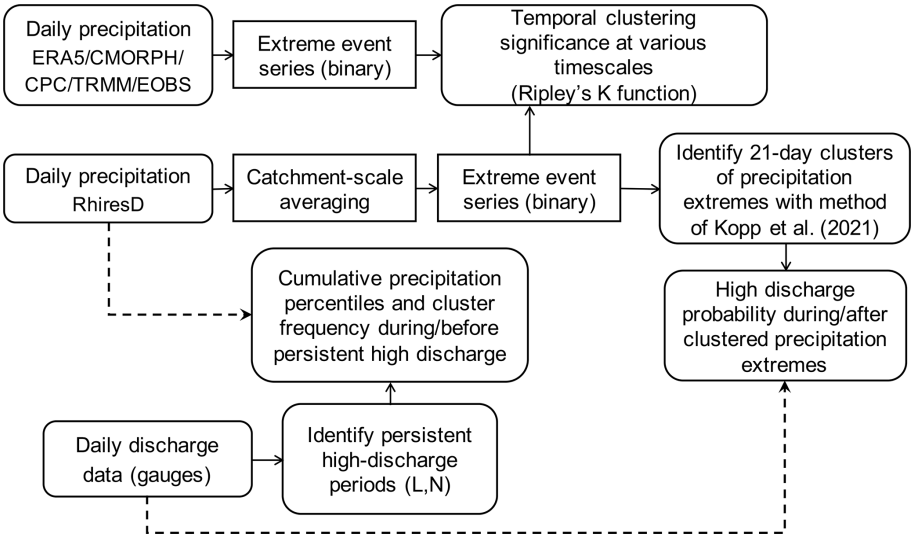

Figure A1. Summary of the data and methodology adopted in this study.

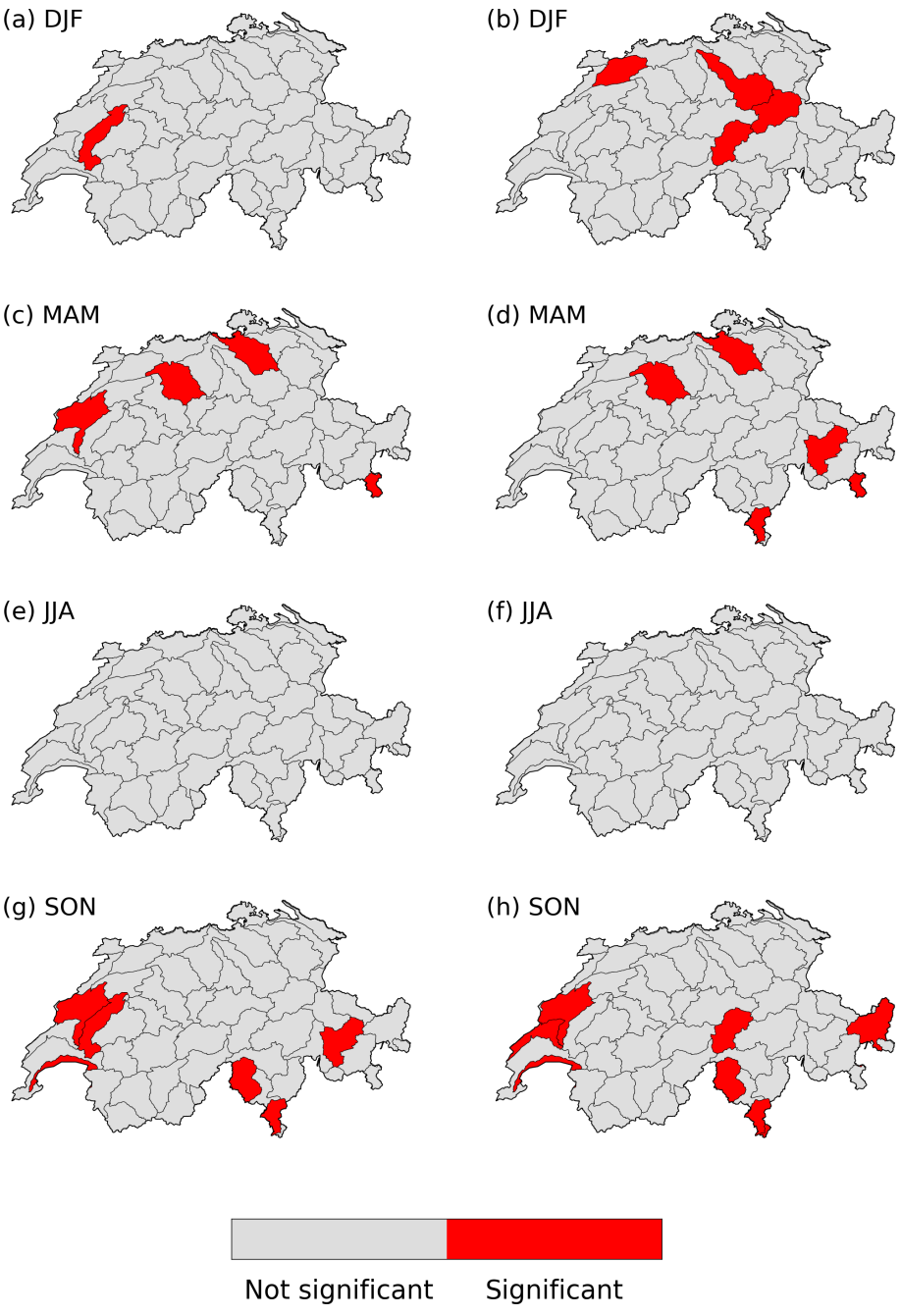

Figure A2. **(a, c, e, g)** Clustering significance in RhiresD for a time window of 5–15 d, in **(a)** DJF, **(c)** MAM, **(e)** JJA and **(g)** SON. **(b, d, f, g)** Same, but for a time window of 25–35 d.

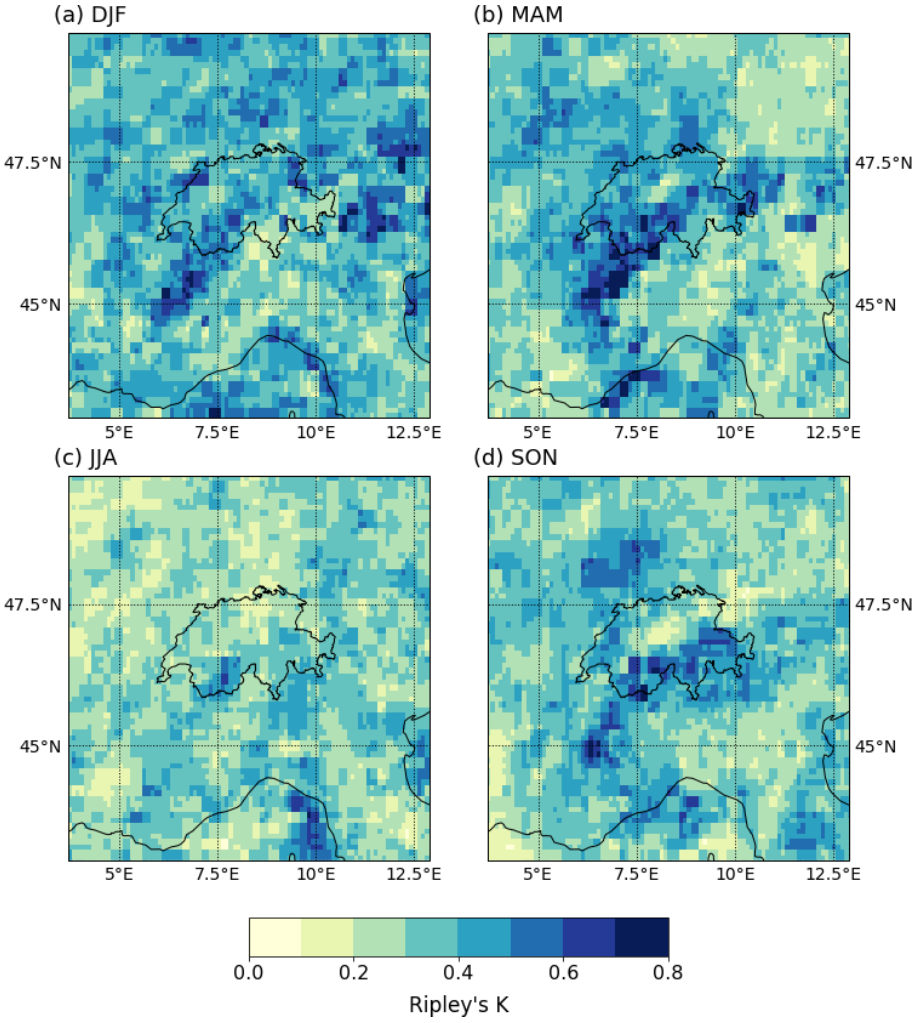

Figure A3. Average Ripley's K value for a 20 d window across ERA5, TRMM, CMORPH, CPC and EOBS in **(a)** DJF, **(b)** MAM, **(c)** JJA and **(d)** SON. For this comparison, all datasets were regridded to the smallest 0.1° EOBS resolution.

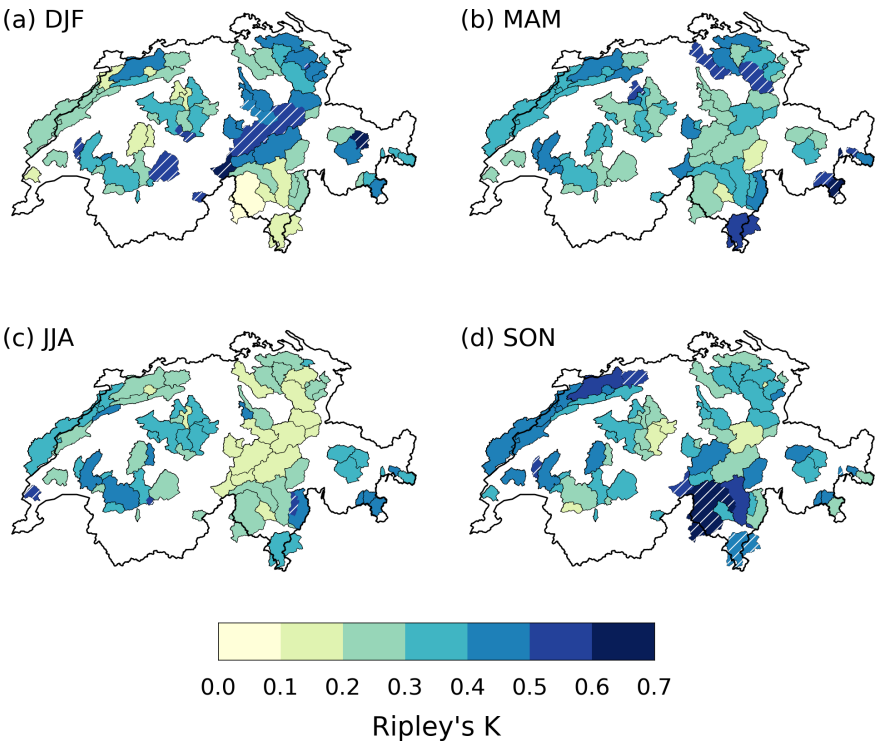

Figure A4. Value of Ripley's K in the RhiresD dataset for a 20 d window, in **(a)** DJF, **(b)** MAM, **(c)** JJA and **(d)** SON, for the 63-catchment partition. Compare with Fig. 4.

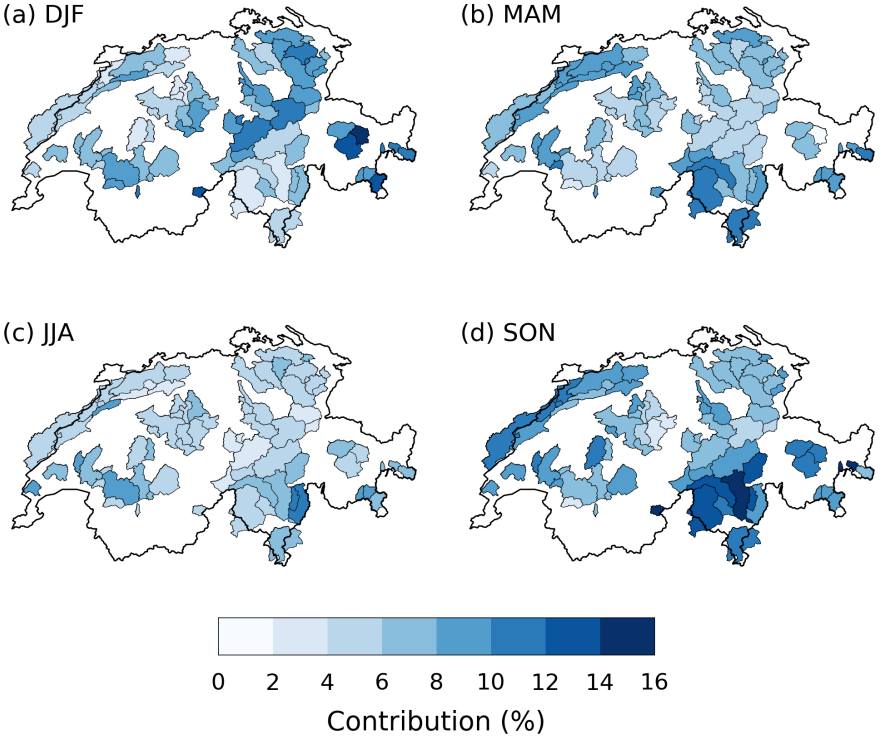

Figure A5. Contribution of 21 d extreme precipitation clusters to seasonal precipitation in RhiresD, in **(a)** DJF, **(b)** MAM, **(c)** JJA and **(d)** SON, for the 63-catchment partition. Compare with Fig. 6.

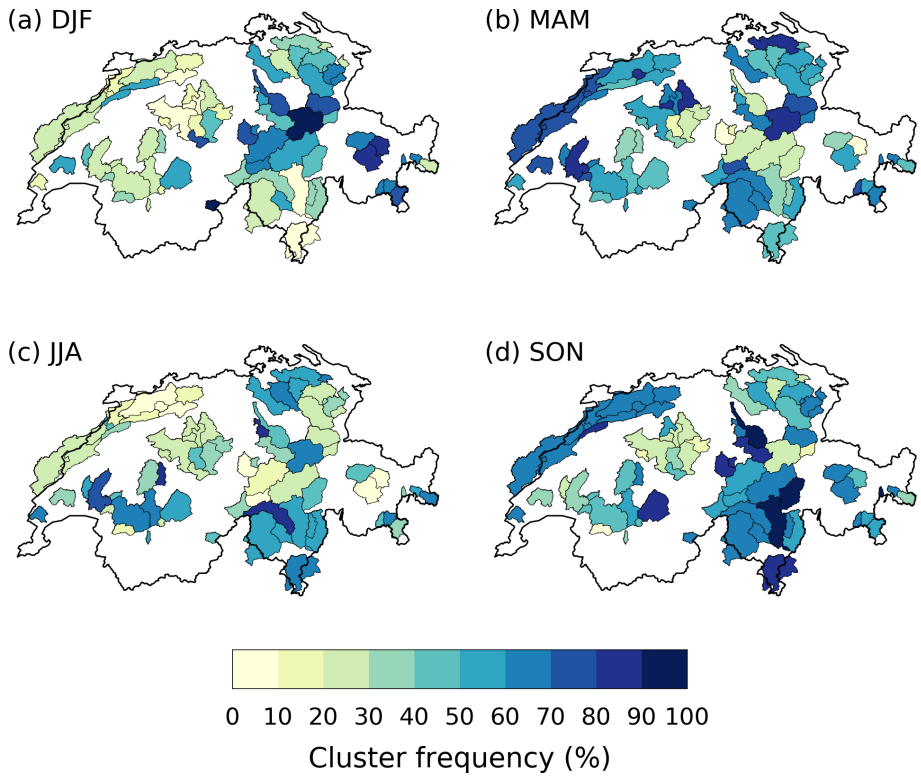

Figure A6. Frequency of extreme precipitation cluster occurrence during extreme 21 d cumulative precipitation events (> 99th percentile) in RhiresD, in **(a)** DJF, **(b)** MAM, **(c)** JJA and **(d)** SON, for the 63-catchment partition. Compare with Fig. 7.

Table A1. List and main characteristics of the 93 gauged Swiss catchments used in this study.

ID	Station	River	Area (km^2)	Mean elev.	Min elev.	Max elev.	Glaciation (%)	Period
2020	Bellinzona	Ticino	1517.5	1679	220	3345	0	Jan 1961–Mar 2016
2033	Ilanz	Vorderrhein	774	2026	685	3557	1.8	Jan 1961–May 2015
2034	Payerne	Broye	415.9	724	368	1574	0	Jan 1961–Dec 2016
2044	Andelfingen	Thur	1701.6	773	354	2431	0	Jan 1961–Dec 2016
2056	Seedorf	Reuss	833.2	2005	432	3598	6.4	Jan 1961–Dec 2016
2070	Emmenmatt	Emme	443	1072	562	2161	0	Jan 1961–Dec 2016
2078	Le Prese	Poschiavino	167.7	2161	962	3875	3.9	Jan 1974–Dec 2017
2084	Ingenbohl	Muota	316.6	1364	425	2731	0	Jan 1961–Dec 2016
2087	Andermatt	Reuss	190.2	2276	1125	3598	2.9	Jan 1961–Jun 2015
2104	Weesen	Linth	1061.5	1580	416	3557	1.6	Jan 1961–Dec 2017
2106	Münchenstein	Birs	887.3	733	256	1424	0	Jan 1961–Dec 2016
2112	Appenzell	Sitter	74.4	1254	445	2431	0	Jan 1961–Dec 2016
2122	Moutier	Birse	185.8	927	493	1424	0	Jan 1961–Apr 2016
2126	Wängi	Murg	80.1	654	456	1113	0	Jan 1961–Mar 2016
2132	Neftenbach	Töss	343.3	659	380	1298	0	Jul 1975–Dec 2016
2141	Tiefencastel	Albula	529	2127	837	3317	0.5	Jan 1961–Mar 2016
2151	Oberwil	Simme	343.7	1639	778	3208	2.4	Jan 1961–Jul 2017
2155	Wiler	Emme	924.1	871	430	2161	0	Jan 1961–Sep 2017
2159	Belp	Gürbe	116.1	849	508	2128	0	Jan 1961–Dec 2016
2160	Broc	Sarine	636.3	1501	674	3207	0	Jan 1961–Dec 2017
2167	Ponte Tresa	Tresa	609.1	805	198	2207	0	Jan 1961–Mar 2016
2176	Zürich	Sihl	342.6	1047	402	2223	0	Jan 1961–Jun 2015
2179	Thörishaus	Sense	351.2	1076	524	2182	0	Jan 1961–Dec 2016
2181	Halden	Thur	1085	914	445	2431	0	Jan 1965–Apr 2016
2185	Chur	Plessur	264.4	1865	545	2923	0	Jan 1961–Dec 2015
2202	Liestal	Ergolz	261.2	591	296	1181	0	Jan 1961–Dec 2016
2203	Aigle	Grande Eau	131.6	1566	384	3167	0.8	Jan 1961–Mar 2016
2210	Ocourt	Doubs	1275.4	960	407	1448	0	Jan 1961–Apr 2016
2219	Oberried	Simme	34.7	2335	1075	3208	22.6	Jan 1961–Apr 2016
2232	Adelboden	Allenbach	28.8	1855	1093	2833	0	Jan 1961–Dec 2016
2256	Pontresina	Rosegbach	66.5	2701	1720	3981	21.7	Jan 1961–Mar 2016
2262	Pontresina	Berninabach	106.9	2608	1783	3981	14.4	Jan 1961–Mar 2016
2270	Combe des Sarrasins	Doubs	998.5	985	553	1448	0	Jan 1961–Mar 2016
2276	Isenthal	Grosstalbach	43.9	1810	767	2961	6.7	Jan 1961–Dec 2016
2299	Erstfeld	Alpbach	20.7	2181	629	3129	19.7	Jan 1961–May 2015
2300	Euthal	Minster	59.1	1352	642	2223	0	Jan 1961–Apr 2016
2303	Jonschwil	Thur	492.9	1027	535	2431	0	Jan 1966–Oct 2017
2304	Zernez	Ova dal Fuorn	55.3	2333	1666	3114	0	Jan 1961–Apr 2016
2305	Herisau	Glatt	16.7	836	624	1145	0	Jan 1961–Apr 2016
2307	Sonceboz	Suze	127.2	1044	634	1595	0	Jan 1961–Oct 2017
2308	Goldach	Goldach	50.4	840	391	1245	0	Feb 1961–Dec 2016
2312	Salmsach	Aach	47.4	476	391	609	0	Apr 1961–Dec 2016
2319	Zernez	Ova da Cluozza	26.9	2361	1468	3115	0	Jul 1961–Apr 2016
2321	Pregassona	Cassarate	75.8	991	272	2198	0	Jun 1962–Apr 2016
2342	Brig	Saltina	76.5	2017	661	3407	2.5	Jan 1966–Dec 2016
2343	Huttwil	Langeten	59.9	765	566	1123	0	Jan 1966–May 2015
2355	Davos	Landwasser	183.7	2223	1453	3180	0	Jan 1967–May 2015
2356	Cavergno	Riale di Calneggia	23.9	1982	645	2866	0	Jan 1967–Mar 2016
2366	La Rösa	Poschiavino	14.1	2286	1707	3012	0	Jan 1970–Apr 2016
2368	Locarno	Maggia	926.9	1534	191	3208	0	Jan 1985–Dec 2017
2369	Yvonand	Mentue	105.3	683	436	946	0	Jan 1971–Jul 2017
2370	Le Noirmont	Doubs	1046.7	985	503	1448	0	Jan 1971–Mar 2016
2372	Mollis	Linth	600.2	1737	427	3557	2.9	Jan 1961–Jun 2015
2374	Mogelsberg	Necker	88.1	962	604	1513	0	Jan 1972–Apr 2016
2386	Frauenfeld	Murg	213.3	596	381	1113	0	Jan 1974–Apr 2016

Table A1. Continued.

ID	Station	River	Area (km^2)	Mean elev.	Min elev.	Max elev.	Glaciation (%)	Period
2409	Eggiwil	Emme	124.4	1283	562	2161	0	Jan 1975–Apr 2016
2412	Vuippens	Sionge	43.4	872	674	1457	0	Feb 1975–Dec 2017
2415	Rheinsfelden	Glatt	417.4	506	340	1105	0	Jan 1976–May 2015
2419	Reckingen	Rhone	214.3	2301	1307	3598	11.8	Jan 1975–Aug 2015
2420	Lumino	Moesa	471.9	1668	229	3169	0	Mar 1980–Apr 2016
2426	Mels	Seez	106.1	1796	469	3073	0	Jan 1966–Sep 2017
2432	Ecublens	Venoge	227.6	694	372	1662	0	Jan 1979–Apr 2016
2434	Olten	Dünnern	233.8	714	390	1383	0	Oct 1977–Jun 2015
2450	Zofingen	Wigger	366.2	662	419	1393	0	Jan 1979–Jun 2015
2461	Magliaso	Magliasina	34.4	927	269	1904	0	Jan 1980–Apr 2016
2468	St. Gallen	Sitter	261.1	1045	445	2431	0	Jul 1980–Apr 2016
2469	Hondrich	Kander	490.7	1846	558	3675	5.1	Aug 1980–Dec 2017
2471	Murgenthal	Murg	183.4	659	410	1123	0	Jun 1980–Dec 2017
2474	Buseno	Calancasca	120.5	1930	503	3169	0.2	Jan 1961–Apr 2016
2477	Zug	Lorze	100.2	822	411	1556	0	Apr 1982–Dec 2017
2478	Soyhières	Birse	569.5	811	380	1424	0	Jun 1982–Dec 2017
2479	Delémont	Sorne	213.9	785	408	1326	0	Jun 1982–Dec 2017
2480	Boudry	Areuse	377.7	1084	427	1573	0	1961/1–2017/6
2481	Buochs	Engelberger Aa	228	1605	432	3137	2.5	Jan 1961–Dec 2016
2486	Vevey	Veveyse	64.5	1108	372	1959	0	Jan 1984–Dec 2017
2487	Werthenstein	Kleine Emme	311.5	1171	525	2290	0	Apr 1984–Dec 2017
2491	Bürglen	Schächen	107.9	1722	436	3221	1.5	Jun 1985–Dec 2017
2493	Gland	Promenthouse	119.8	1035	372	1667	0	Sep 1985–Dec 2017
2494	Pollegio	Ticino	443.8	1794	277	3120	0	May 1986–Dec 2017
2497	Nebikon	Luthern	104.7	754	474	1393	0	Jan 1988–Dec 2017
2498	Castrisch	Glenner	380.9	2014	685	3345	1.1	Jun 1988–Dec 2017
2500	Ittigen	Worble	67.1	678	494	954	0	Jun 1988–Dec 2017
2603	Langnau	Ilfis	187.4	1047	681	2045	0	Apr 1989–Dec 2017
2604	Biberbrugg	Biber	31.9	1008	602	1515	0	Jun 1989–Dec 2017
2605	Lavertezzo	Verzasca	185.1	1663	463	2837	0	Sep 1989–Dec 2017
2607	Oberwald	Goneri	38.4	2378	1353	3120	4	Aug 1990–Dec 2017
2609	Einsiedeln	Alp	46.7	1161	660	1783	0	Feb 1991–Dec 2017
2610	Vicques	Scheulte	72.7	797	419	1292	0	Jan 1992–Dec 2017
2612	Lavertezzo	Riale di Pincascia	44.5	1713	463	2520	0	Jul 1992–Dec 2017
2617	Müstair	Rom	128.5	2188	1167	3196	0	May 1994–Dec 2017
2629	Agno	Vedeggio	99.9	921	198	2198	0	Jan 2004–Dec 2017
2630	Sion	Sionne	27.6	1575	485	3084	0	Oct 2006–Dec 2017
2634	Emmen	Kleine Emme	478.3	1058	425	2290	0	Jan 1961–Jun 2015

Data availability. The RhiresD dataset is provided by MeteoSwiss, the Swiss Federal Office of Meteorology and Climatology. Discharge data were obtained from Switzerland's Federal Office for the Environment. ERA5 reanalysis data for the 1979–2019 period are available from https://cds.climate.copernicus.eu/cdsapp#!/dataset/reanalysis-era5-single-levels?tab=overview (last access: 9 October 2020) (Hersbach et al., 2020). TRMM data can be downloaded at https://doi.org/10.5067/TRMM/TMPA/DAY/7 (Huffman et al., 2016). CMORPH data are provided by NOAA's National Centers for Environmental Information at https://doi.org/10.25921/w9va-q159 (Xie et al., 2019). CPC Global Unified Precipitation data are provided by the NOAA/OAR/ESRL PSL, Boulder, Colorado, USA, from their website at https://psl.noaa.gov/ (last access: 7 October 2020) (Chen et al., 2008).

Code availability. The code used to analyze precipitation series and associated results are available at https://github.com/Quriosity129/Clustering_subseasonal_Switzerland_NHESS (Tuel, 2021).

Author contributions. OM designed and supervised the research. AT designed the research, implemented the code, analyzed the data and provided the figures. AT and OM wrote the paper.

Competing interests. The authors declare that they have no conflict of interest.

Disclaimer. Publisher's note: Copernicus Publications remains neutral with regard to jurisdictional claims in published maps and institutional affiliations.

Special issue statement. This article is part of the special issue "Understanding compound weather and climate events and related impacts (BG/ESD/HESS/NHESS inter-journal SI)". It is not associated with a conference.

Acknowledgements. The authors gratefully acknowledge the Swiss Federal Office of the Environment (FOEN) and Regula Muelchi for the Swiss river discharge data.

Financial support. This research has been supported by the Schweizerischer Nationalfonds zur Förderung der Wissenschaftlichen Forschung (grant no. 178751).

Review statement. This paper was edited by Ricardo Trigo and reviewed by J. Blanchet and one anonymous referee.

References

Aschwanden, H. and Weingartner, R.: Die Abflussregimes der Schweiz, Publikation Gewässerkunde Nr. 65, Geographisches Institut der Universität Bern, Bern, https://doi.org/10.7892/boris.133660, 1985.

BAFU: Umgang mit Naturgefahren – Bericht des Bundesrats in Erfüllung des Postulats 12.4271 Darbellay vom 14.12.2012, Tech. rep., BAFU – Bundesamt für Umwelt, Bern, available at: https://scnat.ch/de/uuid/i/ccaaec15-1b96-57e7-b36d-db5f12864c28-Umgang_mit_Naturgefahren_in_der_Schweiz (last access: 1 October 2021), 2016.

BAFU and WSL: Ereignisanalyse Hochwasser 2005 Teil 2 – Analyse von Prozessen, Massnahmen und Gefahrengrundlagen, Tech. rep., BAFU – Bundesamt für Umwelt, Bern, available at: https://www.bafu.admin.ch/bafu/de/home/themen/naturgefahren/ (last access: 1 October 2021), 2008.

Barton, Y., Giannakaki, P., von Waldow, H., Chevalier, C., Pfahl, S., and Martius, O.: Clustering of Regional-Scale Extreme Precipitation Events in Southern Switzerland, Mon. Weather Rev., 144, 347–369, https://doi.org/10.1175/MWR-D-15-0205.1, 2016.

Blackburn, M., Methven, J., and Roberts, N.: Large-scale context for the UK floods in summer 2007, Weather, 63, 280–288, https://doi.org/10.1002/wea.322, 2008.

Chen, M., Shi, W., Xie, P., Silva, V. B. S., Kousky, V. E., Wayne Higgins, R., and Janowiak, J. E.: Assessing objective techniques for gauge-based analyses of global daily precipitation, J. Geophys. Res., 113, D04110, https://doi.org/10.1029/2007JD009132, 2008.

Coles, S.: An Introduction to Statistical Modeling of Extreme Values, in: Springer Series in Statistics, Springer, London, https://doi.org/10.1007/978-1-4471-3675-0, 2001.

Dacre, H. F. and Pinto, J. G.: Serial clustering of extratropical cyclones: a review of where, when and why it occurs, npj Clim. Atmos. Sci., 3, 48, https://doi.org/10.1038/s41612-020-00152-9, 2020.

Diezig, R. and Weingartner, R.: Hochwasserprozesstypen: Schlüssel zur Hochwasserabschätzung, Wasser Abfall, 4, 18–26, 2007.

Doswell, C. A., Brooks, H. E., and Maddox, R. A.: Flash Flood Forecasting: An Ingredients-Based Methodology, Weather Forecast., 11, 560–581, https://doi.org/10.1175/1520-0434(1996)011<0560:FFFAIB>2.0.CO;2, 1996.

Frei, C. and Schär, C.: A precipitation climatology of the Alps from high-resolution rain-gauge observations, Int. J. Climatol., 18, 873–900, https://doi.org/10.1002/(SICI)1097-0088(19980630)18:8<873::AID-JOC255>3.0.CO;2-9, 1998.

Froidevaux, P. and Martius, O.: Exceptional integrated vapour transport toward orography: an important precursor to severe floods in Switzerland, Q. J. Roy. Meteorol. Soc., 142, 1997–2012, https://doi.org/10.1002/qj.2793, 2016.

Froidevaux, P., Schwanbeck, J., Weingartner, R., Chevalier, C., and Martius, O.: Flood triggering in Switzerland: the role of daily to monthly preceding precipitation, Hydrol. Earth Syst. Sci., 19, 3903–3924, https://doi.org/10.5194/hess-19-3903-2015, 2015.

Giannakaki, P. and Martius, O.: Synoptic-scale flow structures associated with extreme precipitation events in northern Switzerland, Int. J. Climatol., 36, 2497–2515, https://doi.org/10.1002/joc.4508, 2016.

Grams, C. M., Binder, H., Pfahl, S., Piaget, N., and Wernli, H.: Atmospheric processes triggering the central European floods in June 2013, Nat. Hazards Earth Syst. Sci., 14, 1691–1702, https://doi.org/10.5194/nhess-14-1691-2014, 2014.

Guzzetti, F., Peruccacci, S., Rossi, M., and Stark, C. P.: Rainfall thresholds for the initiation of landslides in central and southern Europe, Meteorol. Atmos. Phys., 98, 239–267, https://doi.org/10.1007/s00703-007-0262-7, 2007.

Haylock, M. R., Hofstra, N., Klein Tank, A. M. G., Klok, E. J., Jones, P. D., and New, M.: A European daily high-resolution gridded data set of surface temperature and precipitation for 1950–2006, J. Geophys. Res., 113, D20119, https://doi.org/10.1029/2008JD010201, 2008.

Helbling, A., Kan, C., and Vogt, S.: Dauerregen, Schauer oder Schmelze-welche Ereignisse lösen in der Schweiz die Jahreshochwasser aus?, Wasser Energie Luft, 98, 249–254, 2006.

Hersbach, H., Bell, B., Berrisford, P., Hirahara, S., Horányi, A., Muñoz-Sabater, J., Nicolas, J., Peubey, C., Radu, R., Schepers, D., Simmons, A., Soci, C., Abdalla, S., Abellan, X., Balsamo, G., Bechtold, P., Biavati, G., Bidlot, J., Bonavita, M., Chiara, G., Dahlgren, P., Dee, D., Diamantakis, M., Dragani, R., Flemming, J., Forbes, R., Fuentes, M., Geer, A., Haimberger, L., Healy, S., Hogan, R. J., Hólm, E., Janisková, M., Keeley, S., Laloyaux, P., Lopez, P., Lupu, C., Radnoti, G., Rosnay, P., Rozum, I., Vamborg, F., Villaume, S., and Thépaut, J.: The ERA5 global reanalysis, Q. J. Roy. Meteorol. Soc., 146, 1999–2049, https://doi.org/10.1002/qj.3803, 2020.

Huffman, G. J., Adler, R. F., Bolvin, D. T., Gu, G., Nelkin, E. J., Bowman, K. P., Hong, Y., Stocker, E. F., and Wolff, D. B.: The TRMM Multisatellite Precipitation Analysis (TMPA): Quasi-global, multiyear, combined-sensor precipitation estimates at fine scales, J. Hydrometeorol., 8, 38–55, https://doi.org/10.1175/JHM560.1, 2007.

Huffman, G. J., Bolvin, D. T., Nelkin, E. J., and Adler, R. F.: TRMM (TMPA) Precipitation L3 1 day 0.25 degree × 0.25 degree V7, edited by: Savtchenko, A., Goddard Earth Sciences Data and Information Services Center (GES DISC) [data set], https://doi.org/10.5067/TRMM/TMPA/DAY/7, 2016.

Huntingford, C., Marsh, T., Scaife, A. A., Kendon, E. J., Hannaford, J., Kay, A. L., Lockwood, M., Prudhomme, C., Reynard, N. S., Parry, S., Lowe, J. A., Screen, J. A., Ward, H. C., Roberts, M., Stott, P. A., Bell, V. A., Bailey, M., Jenkins, A., Legg, T., Otto, F. E. L., Massey, N., Schaller, N., Slingo, J., and Allen, M. R.: Potential influences on the United Kingdom's floods of winter 2013/14, Nat. Clim. Change, 4, 769–777, https://doi.org/10.1038/nclimate2314, 2014.

Insua-Costa, D., Miguez-Macho, G., and Llasat, M. C.: Local and remote moisture sources for extreme precipitation: a study of the two catastrophic 1982 western Mediterranean episodes, Hydrol. Earth Syst. Sci., 23, 3885–3900, https://doi.org/10.5194/hess-23-3885-2019, 2019.

Isotta, F. A., Frei, C., Weilguni, V., Perčec Tadić, M., Lassègues, P., Rudolf, B., Pavan, V., Cacciamani, C., Antolini, G., Ratto, S. M., Munari, M., Micheletti, S., Bonati, V., Lussana, C., Ronchi, C., Panettieri, E., Marigo, G., and Vertačnik, G.: The climate of daily precipitation in the Alps: development and analysis of a high-resolution grid dataset from pan-Alpine rain-gauge data, Int. J. Climatol., 34, 1657–1675, https://doi.org/10.1002/joc.3794, 2014.

Joyce, R. J., Janowiak, J. E., Arkin, P. A., and Xie, P.: CMORPH: A Method that Produces Global Precipitation Estimates from Passive Microwave and Infrared Data at High Spatial and Temporal Resolution, J. Hydrometeorol., 5, 487–503, https://doi.org/10.1175/1525-7541(2004)005<0487:CAMTPG>2.0.CO;2, 2004.

Keller, L., Rössler, O., Martius, O., and Weingartner, R.: Delineation of flood generating processes and their hydrological response, Hydrol. Process., 32, 228–240, https://doi.org/10.1002/hyp.11407, 2018.

Köplin, N., Schädler, B., Viviroli, D., and Weingartner, R.: Seasonality and magnitude of floods in Switzerland under future climate change, Hydrol. Process., 28, 2567–2578, https://doi.org/10.1002/hyp.9757, 2014.

Kopp, J., Rivoire, P., Ali, S. M., Barton, Y., and Martius, O.: A novel method to identify sub-seasonal clustering episodes of extreme precipitation events and their contributions to large accumulation periods, Hydrol. Earth Syst. Sci., 25, 5153–5174, https://doi.org/10.5194/hess-25-5153-2021, 2021.

Mailier, P. J., Stephenson, D. B., Ferro, C. A. T., and Hodges, K. I.: Serial Clustering of Extratropical Cyclones, Mon. Weather Rev., 134, 2224–2240, https://doi.org/10.1175/MWR3160.1, 2006.

Martius, O., Zenklusen, E., Schwierz, C., and Davies, H. C.: Episodes of alpine heavy precipitation with an overlying elongated stratospheric intrusion: a climatology, Int. J. Climatol., 26, 1149–1164, https://doi.org/10.1002/joc.1295, 2006.

Martius, O., Sodemann, H., Joos, H., Pfahl, S., Winschall, A., Croci-Maspoli, M., Graf, M., Madonna, E., Mueller, B., Schemm, S., Sedláček, J., Sprenger, M., and Wernli, H.: The role of upper-level dynamics and surface processes for the Pakistan flood of July 2010, Q. J. Roy. Meteorol. Soc., 139, 1780–1797, https://doi.org/10.1002/qj.2082, 2013.

Medina, S. and Houze, R. A.: Air motions and precipitation growth in Alpine storms, Q. J. Roy. Meteorol. Soc., 129, 345–371, https://doi.org/10.1256/qj.02.13, 2003.

Merz, R., Blöschl, G., and Parajka, J.: Spatio-temporal variability of event runoff coefficients, J. Hydrol., 331, 591–604, https://doi.org/10.1016/j.jhydrol.2006.06.008, 2006.

Muelchi, R., Rössler, O., Schwanbeck, J., Weingartner, R., and Martius, O.: An ensemble of daily simulated runoff data (1981–2099) under climate change conditions for 93 catchments in Switzerland (Hydro-CH2018-Runoff ensemble), Geosci. Data J., https://doi.org/10.1002/gdj3.117, in press, 2021a.

Muelchi, R., Rössler, O., Schwanbeck, J., Weingartner, R., and Martius, O.: River runoff in Switzerland in a changing climate – runoff regime changes and their time of emergence, Hydrol. Earth Syst. Sci., 25, 3071–3086, https://doi.org/10.5194/hess-25-3071-2021, 2021b.

Nied, M., Pardowitz, T., Nissen, K., Ulbrich, U., Hundecha, Y., and Merz, B.: On the relationship between hydrometeorological patterns and flood types, J. Hydro., 519, 3249–3262, https://doi.org/10.1016/j.jhydrol.2014.09.089, 2014.

Panziera, L., Gabella, M., Zanini, S., Hering, A., Germann, U., and Berne, A.: A radar-based regional extreme rainfall analysis to derive the thresholds for a novel automatic alert system in Switzerland, Hydrol. Earth Syst. Sci., 20, 2317–2332, https://doi.org/10.5194/hess-20-2317-2016, 2016.

Panziera, L., Gabella, M., Germann, U., and Martius, O.: A 12-year radar-based climatology of daily and sub-daily extreme precip-

itation over the Swiss Alps, Int. J. Climatol., 38, 3749–3769, https://doi.org/10.1002/joc.5528, 2018.

Paschalis, A., Fatichi, S., Molnar, P., Rimkus, S., and Burlando, P.: On the effects of small scale space-time variability of rainfall on basin flood response, J. Hydrol., 514, 313–327, https://doi.org/10.1016/j.jhydrol.2014.04.014, 2014.

Piaget, N.: Meteorological characterizations of extreme precipitation and floods in Switzerland, Doctoral thesis, ETH Zürich, Zurich, https://doi.org/10.3929/ethz-a-010542049, 2015.

Piaget, N., Froidevaux, P., Giannakaki, P., Gierth, F., Martius, O., Riemer, M., Wolf, G., and Grams, C. M.: Dynamics of a local Alpine flooding event in October 2011: moisture source and large-scale circulation, Q. J. Roy. Meteorol. Soc., 141, 1922–1937, https://doi.org/10.1002/qj.2496, 2015.

Pinto, J. G., Bellenbaum, N., Karremann, M. K., and Della-Marta, P. M.: Serial clustering of extratropical cyclones over the North Atlantic and Europe under recent and future climate conditions, J. Geophys. Res.-Atmos., 118, 12476–12485, https://doi.org/10.1002/2013JD020564, 2013.

Priestley, M. D. K., Pinto, J. G., Dacre, H. F., and Shaffrey, L. C.: The role of cyclone clustering during the stormy winter of 2013/2014, Weather, 72, 187–192, https://doi.org/10.1002/wea.3025, 2017.

Priestley, M. D. K., Dacre, H. F., Shaffrey, L. C., Hodges, K. I., and Pinto, J. G.: The role of serial European windstorm clustering for extreme seasonal losses as determined from multi-centennial simulations of high-resolution global climate model data, Nat. Hazards Earth Syst. Sci., 18, 2991–3006, https://doi.org/10.5194/nhess-18-2991-2018, 2018.

Raymond, C., Horton, R. M., Zscheischler, J., Martius, O., AghaKouchak, A., Balch, J., Bowen, S. G., Camargo, S. J., Hess, J., Kornhuber, K., Oppenheimer, M., Ruane, A. C., Wahl, T., and White, K.: Understanding and managing connected extreme events, Nat. Clim. Change, 10, 611–621, https://doi.org/10.1038/s41558-020-0790-4, 2020.

Ripley, B. D.: Spatial Statistics, Wiley Series in Probability and Statistics, John Wiley & Sons, Inc., Hoboken, NJ, USA, https://doi.org/10.1002/0471725218, 1981.

Rivoire, P., Martius, O., and Naveau, P.: A comparison of moderate and extreme ERA-5 daily precipitation with two observational data sets, Earth and Space Science Open Archive ESSOAr, https://doi.org/10.1175/JCLI-D-15-0710.1, 2021.

Rössler, O., Froidevaux, P., Börst, U., Rickli, R., Martius, O., and Weingartner, R.: Retrospective analysis of a nonforecasted rain-on-snow flood in the Alps – a matter of model limitations or unpredictable nature?, Hydrol. Earth Syst. Sci., 18, 2265–2285, https://doi.org/10.5194/hess-18-2265-2014, 2014.

Stucki, P., Rickli, R., Brönnimann, S., Martius, O., Wanner, H., Grebner, D., and Luterbacher, J.: Weather patterns and hydro-climatological precursors of extreme floods in Switzerland since 1868, Meteorol. Z., 21, 531–550, https://doi.org/10.1127/0941-2948/2012/368, 2012.

Swiss Re: Floods in Switzerland – an underestimated risk, Tech. rep., Swiss Re, Zurich, available at: https://www.planat.ch/fileadmin/PLANAT/planat_pdf/alle_2012/2011-2015/Swiss_Re__Hg__2012_-_Floods_in_Switzerland.pdf (last access: 1 October 2021), 2012.

Tuel, A.: Clustering_subseasonal_Switzerland, Github [code], https://github.com/Quriosity129/Clustering_subseasonal_Switzerland_NHESS/, last access: 1 October 2021.

Tuel, A. and Martius, O.: A global perspective on the sub-seasonal clustering of precipitation extremes, Weather Clim. Extrem., 33, 100348, https://doi.org/10.1016/j.wace.2021.100348, 2021.

Umbricht, A., Fukutome, S., Liniger, M. A., Frei, C., and Appenzeller, C.: Seasonal variation of daily extreme precipitation in Switzerland, Tech. rep., MeteoSwiss, 97, 122 pp., available at: https://www.meteoschweiz.admin.ch/home/service-und-publikationen/publikationen.subpage.html/de/data/publications/2013/6/seasonal-variation-of-daily-extreme-precipitation-in-switzerland.html (last access: 1 October 2021), 2013.

van Oldenborgh, G. J., Stephenson, D. B., Sterl, A., Vautard, R., Yiou, P., Drijfhout, S. S., von Storch, H., and van den Dool, H.: Drivers of the 2013/14 winter floods in the UK, Nat. Clim. Change, 5, 490–491, https://doi.org/10.1038/nclimate2612, 2015.

Villarini, G., Smith, J. A., Vitolo, R., and Stephenson, D. B.: On the temporal clustering of US floods and its relationship to climate teleconnection patterns, Int. J. Climatol., 33, 629–640, https://doi.org/10.1002/joc.3458, 2013.

Vitolo, R., Stephenson, D. B., Cook, I. M., and Mitchell-Wallace, K.: Serial clustering of intense European storms, Meteorol. Z., 18, 411–424, https://doi.org/10.1127/0941-2948/2009/0393, 2009.

Wilks, D.: Statistical Methods in the Atmospheric Sciences, 4th Edn., Elsevier, https://doi.org/10.1016/C2017-0-03921-6, 2019.

Wilks, D. S.: "The Stippling Shows Statistically Significant Grid Points": How Research Results are Routinely Overstated and Overinterpreted, and What to Do about It, B. Am. Meteorol. Soc., 97, 2263–2273, https://doi.org/10.1175/BAMS-D-15-00267.1, 2016.

Xie, P., Joyce, R., Wu, S., Yoo, S.-H., Yarosh, Y., Sun, F., Lin, R., and NOAA CDR Program: NOAA Climate Data Record (CDR) of CPC Morphing Technique (CMORPH) High Resolution Global Precipitation Estimates, Version 1, NOAA National Centers for Environmental Information [data set], https://doi.org/10.25921/w9va-q159, 2019

Yang, Z. and Villarini, G.: Examining the capability of reanalyses in capturing the temporal clustering of heavy precipitation across Europe, Clim. Dynam., 53, 1845–1857, https://doi.org/10.1007/s00382-019-04742-z, 2019.